2.3 Experimental research on wood anatomical structure

Material properties are most structure dependent, especially for anisotropic materials like wood. Thermal conductivity of wood is an example of a structure-dependent material property. Several studies have found the influence of wood structure on thermal conductivity (Wangaard 1940, 1943, Siau 1968, 1995, Kamke and Zylkowski 1989, and Suleiman et.al 1999). Significant factors of the structure include cell walls, porosity, wood rays, and sub-microscopic structure of cell walls, such as microfibril orientation.

An obvious representation of a wood anisotropic characteristic is the differential shrinkage during drying. It has been found that wood shrinks two to five times greater in the tangential direction to the growth ring than it does in the radial direction on the cross section of wood. This differential shrinkage has been studied for years and reasons were found to be all related to the wood structure, such as earlywood/latewood arrangement, wood rays, cell wall thickness, and microfibril orientation (Pentoney 1952, Skaar 1988). Heat and mass transfer in the radial and tangential direction in the wood lumber drying process has been the most interesting topic for the wood products industry. The influence of structure on heat and mass transportation in the two directions is a study that remains to be done. This research is focusing on the influence of wood structure on the heat transfer process in the radial and tangential direction.

Thermal conductivity plays a most important role in heat transfer. Wood thermal conductivity represents the resultant conductivity of the wood substance present as well as that of the included air and moisture (Wangaard 1940). So the thermal conductivity property related to wood anatomical structures will be studied in the radial and tangential direction to examine the possible influence on the heat transfer in the two directions and to theoretically estimate the thermal conductivity values.

2.3.1 Materials and Methods

2.3.1.1 Sample preparation

The purpose of this test is to observe the general structure difference in the radial and tangential directions. Based on the microscope observation, a geometric model for estimating the effective thermal conductivity in the two directions will be set up. Since wood is a very complicated structure, in order to represent the structure differences among the species, two softwood species and one hardwood species were selected in this study. The two softwood

species are southern yellow pine (*Pinus spp*.) and Scots pine (*P. sylvestris*), which are, respectively, the most popular softwood construction lumber utilized in America and Europe. The hardwood species selected in the study is the soft maple (*Acer rubrum*), which contains a significant amount of wood rays.

Southern yellow pine and soft maple were collected and examined locally (Blacksburg, Virginia, U.S.). Scots pine materials were all collected from the EMPA, Switzerland (The Swiss Federal Institute for Material Testing). Microscopic observation of Scots pine was also done at EMPA, Switzerland.

Approximate 6×6×6 mm cubes were cut from the three species of wood materials. A clear, smooth cutting surface on the samples is important to the microscopic observation. Preliminary tests showed that the cut surface with a razor blade was better than the surface cut by a microtome for the Scanning Electron Microscope (SEM) observation. In order to get a smooth cut face with the razor blade, samples had to be saturated before the cutting. All the cubes were fully saturated in a special vacuum container before they were surfaced. After smoothing one surface (cross section of wood) on the cubes with razor blades, the sample cubes were subjected to the drying process to get rid of all of moisture in the samples because the Scanning Electron Microscope requires completely dry samples to work in a vacuum environment. Southern yellow pine and soft maple samples were dried in an ordinary oven with the temperature set at 103°C. They were taken out from the oven after being dried for 24 hours. Scots pine samples were dried in a vacuum dryer with the temperature of 40°C. The samples were dried for about 12 hours before they were prepared for the SEM observation. The dried samples were mounted on the SEM sample holders and sputter coated with platinum or gold and then inserted into the Scanning Electron Microscope for observation. Southern yellow pine and maple samples were observed with the AMRAY 1800 Scanning Electron Microscope at Forest Products Brooks Center of Virginia Tech, and Scots pine samples were observed in the field emission scanning electron microscope (FE-SEM) JEOL-6300-F at EMPA, Switzerland. In order to fulfil the comparison of the cell wall percentage on wood cross section before and after drying, Scots pine saturated samples were examined using the Philips XL30-FEG Environmental Scanning Electronic Microscope with field emission cathode (FE-ESEM) at the University of Basel, Switzerland. This ESEM equipment eliminates the high vacuum in the microscope chamber of conventional SEMs, and uses a high pressure gaseous atmosphere for study of wet or oily samples. This allows the observation in a normal environment, i.e. in a humid atmosphere with normal air pressure. So, the

cell wall thickness of the radial and tangential wall could be measured under the 'original' wet condition to compare with the dry sample cell wall quantity.

Two to four cubes for each species were prepared for each test. The smooth, clear cut cross sections of the three species were observed under the SEM and ESEM for examining the gross structure and the cell wall percentage in the radial and tangential direction.

2.3.1.2 Anatomical structure observation

Transverse sections of the three species were examined using the Scanning Electron Microscope. Twenty clear images were selected from the four cubes of southern yellow pine, 10 of which were from the earlywood area, and the other 10 were from the latewood area. Figure 2.11 and Figure 2.12 show the southern yellow pine earlywood and latewood structure selected from the 20 images. Same amount of images were obtained from the soft maple cube samples. Earlywood and latewood structure of soft maple are shown in Figure 2.13 and 2.14.

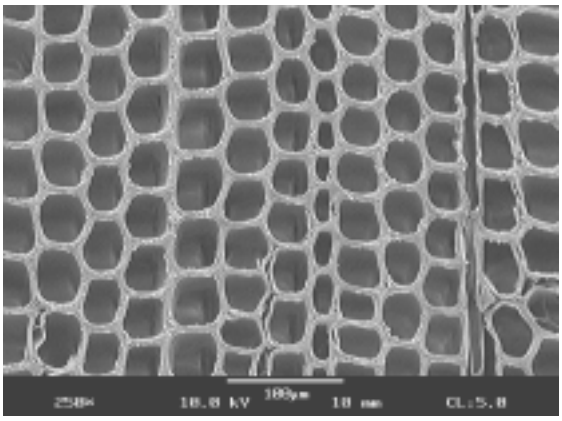

Figure 2. 1 Southern yellow pine earlywood image.

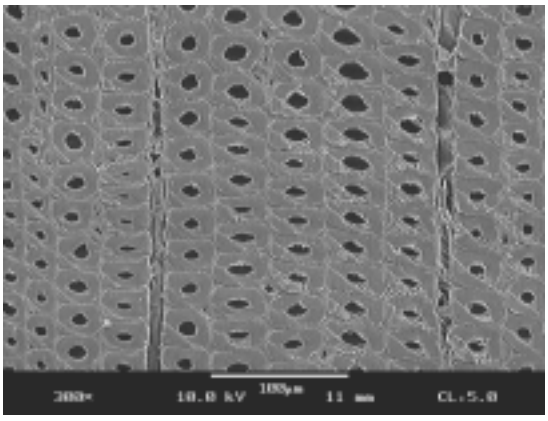

Figure 2. 2 Southern yellow pine latewood image.

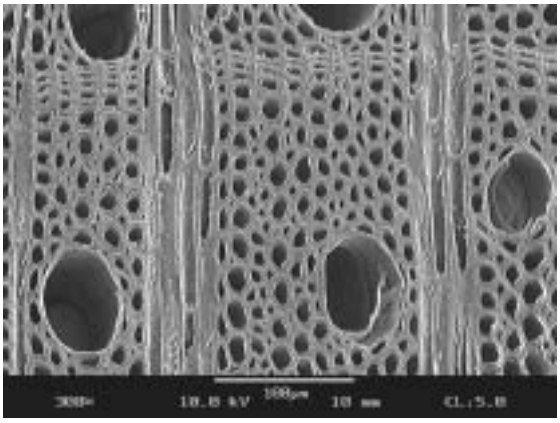

Figure 2. 3 Soft maple latewood image.

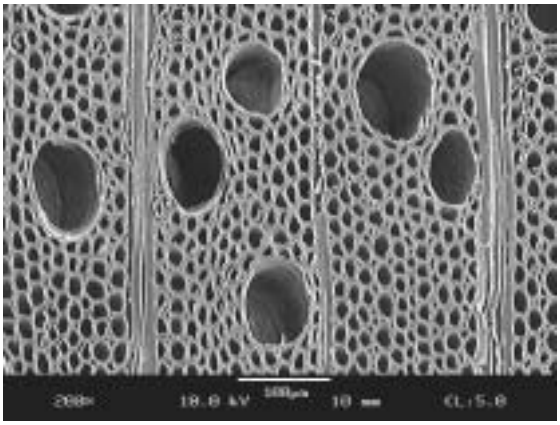

Figure 2. 4 Soft maple earlywood image.

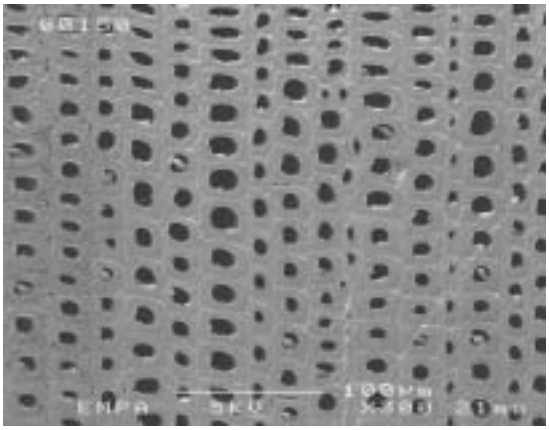

Figure 2. 5 Scots pine latewood dry condition image.

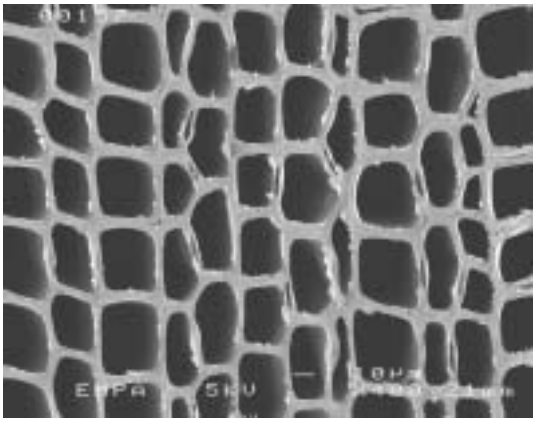

Figure 2. 6 Scots pine earlywood dry image.

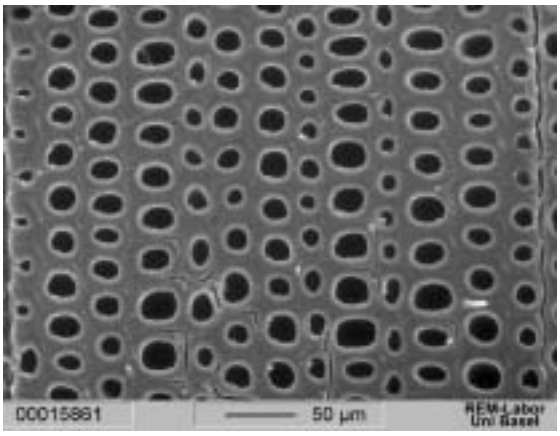

Figure 2. 7 Scots pine latewood green condition image.

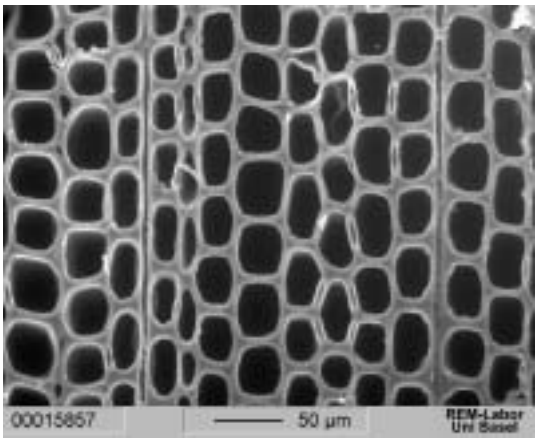

Figure 2. 8 Scots pine earlywood green image.

Ten images for Scots pine dry earlywood and latewood structure were obtained from the two Scots pine sample cubes by the SEM, five of which were earlywood images, and the other five images were latewood structure. The same amount of images were obtained from the Scots pine saturated samples by the ESEM. Examples of the earlywood and latewood structure of Scots pine dry sample and wet sample are shown in Figures 2.15 -- 2.18.

After all the required images were collected, they were loaded into image analysis software for measurement. Ten random lines were drawn on each image horizontally and vertically. (Horizontal direction on the image correspond to the tangential direction of wood structure, and vertical direction corresponds to the radial direction). Cell wall percent on each line were measured and calculated. The results are shown in the next section.

2.3.2 Results and Discussion

One obvious gross structure on the cross section of wood is the growth ring. Tree growth is characterized as fast growing in early spring and slowing down in late summer before ceasing in the fall. This growing style gives wood structure an alternating arrangement of earlywood and latewood on the cross section. For softwood species, in earlywood, cells are big with thin cell walls and large lumens, while in latewood, cells are relatively small with very thick walls and small lumens. Three categories are defined for hardwood species – ring porous, semi-ring porous and diffuse porous, depending on the big thin walled vessels distribution. Maple is a diffuse porous hardwood species. The latewood on the diffuse porous hardwood species is characterized with a light band at the end of each annual ring, which consists of thick walled parenchyma and fibers. Due to this structure difference between the earlywood cells and latewood cells, the physical and mechanical properties of earlywood and latewood are very different. The amount of earlywood and latewood on the cross section of wood varies from ring to ring and from sample to sample. The overall wood physical and mechanical properties are related to the amount of earlywood and latewood contained in wood. So the amount and arrangement of earlywood and latewood are important to the geometric model proposed in the next section for the thermal conductivity in the transverse direction. The total percentage of earlywood and latewood on each testing sample should be measured individually as the input for the model estimation of thermal conductivity in the validation tests. The simplified structure for the softwoods can be displayed as Figure 2.19. The earlywood and latewood are in parallel arrangement in the tangential direction, and in series arrangement for the radial direction. It can be further modified or simplified by moving all the latewood together on the top, and all the earlywood together at the bottom. The

simplified structure model (Figure 2.19) here seems to assume the square shape for individual cells and uniform size of earlywood and latewood cells respectively. But later, in the geometric model proposed for deriving the transverse thermal conductivity, it was not limited to this assumption.

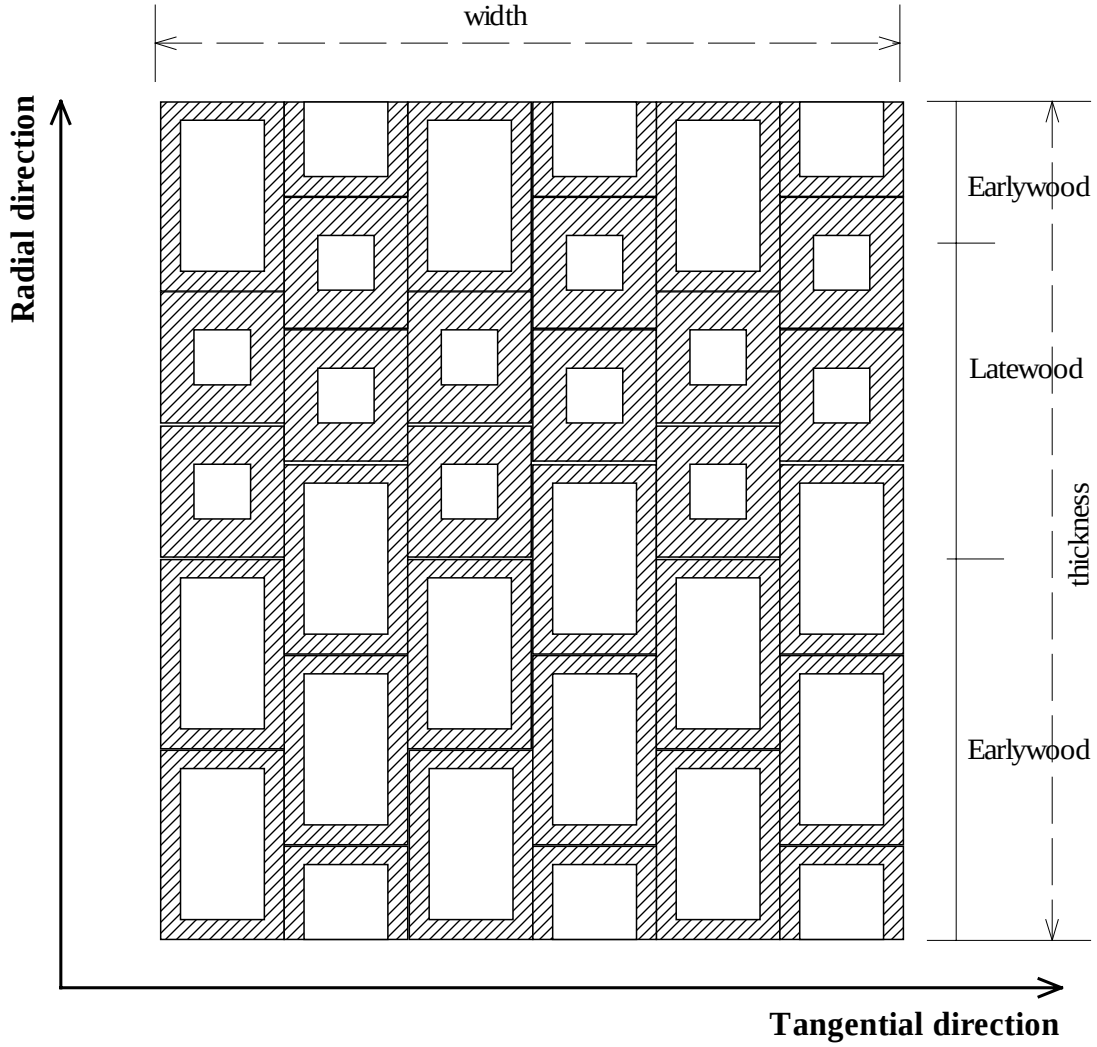

Figure 2. 9 Simplified structure model for the softwood species.

The structure of hardwoods may not be as neat or uniform as softwoods, but the earlywood and latewood arrangement in the two directions on the cross section is the same as in the softwood model. The simplified structure model proposed for the softwoods can also be applied to the hardwood species. The amount or percentage of latewood on the cross section for the specific maple species is very small and doesn't vary much from one growth ring to another or

from one sample to another sample. So a fixed latewood percentage will be used later as the input of model estimation for soft maple transverse thermal conductivities.

From the images of the two softwood species ---- southern yellow pine (Figure 2.11 and 2.12) and Scots pine (Figure 2.15 and 2.16), it was observed that the arrangement of individual cells (most of them are longitudinal tracheids) is neat for both earlywood and latewood. They are aligned perfectly in the radial direction with several small rays between the aligned tracheids. The rays in softwood species are very narrow with only one cell wide. The cells are arranged alternately in the tangential direction. Among all the randomly-drawn lines in the tangential direction across the image, there was no one single line with all the cell wall occupied. It was always cell wall and cell lumen alternately arranged. But in the radial direction, there was a part of the image with full cell wall running through the whole radial lines (vertical lines on the image). This part is the side walls of radially aligned cells. Based on this observation, the geometric model (next section) for the transverse thermal conductivity can be proposed. Since the effective thermal conductivity of wood represents the resultant thermal conductivity of the major components in wood ----the cell wall substance and air in the cell lumen, the arrangement and the amount of the cell wall in the two directions is the basis for setting up the wood thermal conductivity geometric model.

The hardwood species, maple, doesn't have as uniform a structure as the softwood species because of the randomly dispersed vessels, which are extremely large compared to the other types of cells (see in Figure 2.13 and 2.14). So the cell wall is arranged alternately with the lumen in both radial and tangential direction (horizontal and vertical direction on the image). The wood ray is a significant part in the maple gross structure on the cross section. The axis of a ray parenchyma runs perpendicular to the axis of the wood grain. Rays form strands extended radially on the transverse plane. The microfibrils in the ray walls are relatively parallel to the cell axis, thus perpendicular to the microfibrils in the longitudinal cell walls. This different orientation for the two types of cells is important and will be shown as two separated components in the soft maple geometric model proposed in the next section. The ray percentage on the cross section is an important parameter for the hardwood species geometric model.

The averaged cell wall percent in the radial and tangential direction for the three species were measured, calculated and concluded in table 2.1, 2.2, and 2.3. The side wall percentage in the radial direction for the softwood species ----southern yellow pine and Scots pine, were also

measured and shown in *Table 2.1* and *Table 2.2*. Ray percentage on the maple cross section was measured separately and shown in *Table 2.3*.

Table 2. 1 The anatomical structure measurement result for southern yellow pine

	Earlywood			Latewood		
	radial	tangential	side wall	radial	tangential	side wall
cell wall percent	***16.49%***	***31.50%***	***15.94%***	***44.37%***	***66.94%***	***50.77%***

Table 2. 2 The anatomical structure measurement result for Scots pine.

	Earlywood			Latewood		
	radial	tangential	side wall	radial	tangential	side wall
cell wall percent	***13.69%***	***31.46%***	***13.50%***	***52.98%***	***71.51%***	***50.83%***

Table 2. 3 The anatomical structure measurement result for soft maple.

	Earlywood cell wall		Latewood cell wall		rays
	radial	tangential	radial	tangential	
percent	***38.71%***	***50.36%***	***52.05%***	***72.01%***	***14.62%***

These measurements were obtained by using image analysis software. Each result was averaged from 50 (for Scots pine) or 100 (for SYP and maple) measurements. The original data were listed in the Table A-1 to A-17 in the Appendix A. The large number of the data obtained provides confidence to assume a normal distribution of these data (although some of these data didn't follow the normal distribution very well after the normality tests by the statistical software MiniTab). Based on the normal distribution assumption, the statistical ANOVA can be applied on these data to examine the significant difference among the species, between the earlywood and latewood, and between the radial and tangential direction.

Results in the above three tables are averages taken among the data obtained from different images. So the image effect on each of the averaged results should be examined at the same time as examining the significant factors. The *generalized random block design (GRBD)* statistical model analysis was employed here to examine the influence of the direction (radial vs. tangential) for all of the three species, with images being considered as the blocks and the direction being considered as the treatment when running the *GRBD* model in the SAS software. The results from SAS software are shown in Appendix A, Tables A.22-A.27. The results showed that the cell wall percentages in the tangential direction were all significantly greater than the cell wall percentages in the radial direction for both earlywood and latewood of all three species. This was anticipated and could be a factor for the different physical properties in the two directions found before. For example, the differential shrinkage in the two directions may be due to the different cell wall substances in the two directions. More cell wall substances in the tangential direction gives more shrinkage in the tangential direction than the radial since the cell wall plays the first important roll in the drying shrinkage. The different amount of cell wall substances in the two directions was expected by the author before the tests, which was also the motivation for this study. If there is a difference for the cell wall substance in the radial and tangential directions, the heat transfer property -- thermal conductivity, may show differences in the two directions too, because heat transportation in wood mainly goes through the cell wall part. Based on the observation for wood anatomical structure from the microscope images, the geometric models for deriving the effective thermal conductivity in two different directions will be set up differently in the next section.

The image (block) effect was examined at the same time examining the direction (radial vs. tangential) affect by the *GRBD* statistic analysis. Results (Table A-22 to A-27) showed that some of the data that were measured may be affected by obtaining from different images, but not as significantly as by the direction (radial vs. tangential) factor. The image (blocks in the randomized experimental design) effect can be eliminated if the images are taken carefully and precisely within earlywood or latewood area.

To examine the difference of these parameters between the two softwood species and among three species (including one hardwood species), one averaged value from each image for each parameter was used. The cell wall percentage in radial and tangential direction from the three species was compared by the *randomized complete block design (with subsamplings)* statistical model. The radial and tangential direction is considered as the block in the model and the species is set as the treatment when running the models in SAS software. The statistic test was

run on data obtained from earlywood and latewood separately. The difference between the two softwood species was examined first, then followed by the examination of the difference among the three species. The results are shown in Tables A-28 to A-31 of the Appendix A. No significant difference of the cell wall substance between the two pine species was found. Test among the three species (including maple species) showed that only in the earlywood area, there is a little significant difference for the cell wall substance among the three species (with $p=0.0152$). This was caused by introducing the hardwood species--maple into the statistical test because the same test made on the two softwood species before didn't show the difference (with $p=0.1055$). Maple earlywood has a lot more cell wall substance in the tangential direction than the two softwood pine species. To draw a conclusion on the difference of cell wall substance among the species (including both softwoods and hardwoods), more tests and more species need to be examined.

All the data examined so far are the ones obtained from the dry wood samples of the three species. Cell wall substance will be swollen if there is moisture in wood. So the cell wall percentage in the two directions obtained from the wet samples was suspected to be different from the values obtained from the dry samples. Only Scots pine cell wall percentage under the wet condition was measured on the images obtained from the Environmental Scanning Electron Microscope. The data from Scots pine were analyzed by the *randomized complete block design (with subsamplings)* model to examine the significant difference of cell wall percentages in radial and tangential directions between the dry and green samples. The results (Table A-32 to A-33 in Appendix A) from ANOVA show that there is no significant difference between the dry and wet samples for the cell wall percentage in latewood area. But there is significant difference between the two sets of data for the earlywood cell wall percentage both in radial and tangential direction. This is explained by the fact that latewood cells are small with thick walls and small lumens, while the earlywood cells are big with very thin walls and much bigger lumens. Although thick walls may give latewood cells more swelling than the thin-walled earlywood cells, the less void or lumen space in the latewood area prevents the swelling. In the earlywood, although the cell walls of the earlywood tracheids themselves may not be able to swell as much as the latewood tracheids, they can be forced to swell with their neighbors --latewood tracheids, to some extent. And the large lumens provide the space for the cell walls to swell. So the cell walls in the earlywood significantly increased for the wet samples. Later, in the model estimation process (next section), the cell wall percentage parameters required in the model inputs have to be distinguished for the dry wood model and the wet wood model.

2.4 Analytical research on wood transverse thermal conductivity modeling

The geometric models for the thermal conductivity in the radial and tangential directions proposed in this study are based on the consideration of earlywood/latewood percentage and arrangement, cell wall percentage and arrangement in the two directions. The latewood percentage and cell wall percentage are the two major factors for the specific gravity of wood species and individual samples. This made the current model a closer representation of the wood structure influence on the properties than the models proposed by Kollmann (1956) and Siau (1968) before. In the previous geometric models (see in *Background* part), single cells were chosen as the structure basis for the geometric model, which didn't account for earlywood and latewood interaction or the different arrangement in the different directions. The geometric models proposed below not only take the individual cell structure into consideration, but also the gross structure on wood cross section.

Since the microscope structure of softwoods doesn't vary significantly from species to species, except for the specific gravity, which came from the different amount of cell wall percentage and latewood percentage in the samples, the geometrical model for deriving the thermal conductivity is the same for all the softwood species, only with different parameters (such as cell wall percentage) for different species in the model.

The structure of hardwoods is much different from softwood species. The geometric model for the maple species will be set up differently from that for the two pine species.

2.4.1 Model development

2.4.1.1 Geometric model for softwoods

Geometric models were set up based on the microscopic observations. Assumptions were made for setting up the models:

- cell wall, cell lumen arrangement and amount percentage in the radial and tangential direction measured from the microscopic test represent the heat transfer path in the two directions;

- shrinkage/swelling in the cell wall is not considered in the model before reaching the FSP. Cell wall percentage does not change between moisture content (MC) of 0% and less

than 30%. When FSP (MC of 30%) is reached, cell wall percentages are increased to new values for both radial and tangential directions due to the fully saturation wit bound water in the cell wall;

- Earlywood/Latewood are separated for the heat transportation in the geometric models developed due to the different specific gravity of earlywood and latewood;

Model development starts from the softwoods since the structure of softwoods is relatively uniform. The simplified and modified structure of softwoods was shown in the last section (Figure 2.19). It was shown that earlywood and latewood were arranged in parallel for the tangential direction and in series for the radial direction. After measuring the total cell wall percentage in the radial and tangential direction for both earlywood and latewood, the geometric model can be set up by moving all the cell walls together on one side, and all the lumens together on the other side. Within each earlywood and latewood, we found that the cell wall and cell lumen were arranged in series for tangential direction, while for radial direction, side walls were arranged in parallel with the series layout of the cross walls (top and bottom walls of cells) and cell lumen. The geometric models for the general softwoods radial and tangential structures are shown in Figure 2.20 and Figure 2.21. The cell wall percentage for each part in each direction was obtained from the anatomical structure measurement for each species from the previous section.

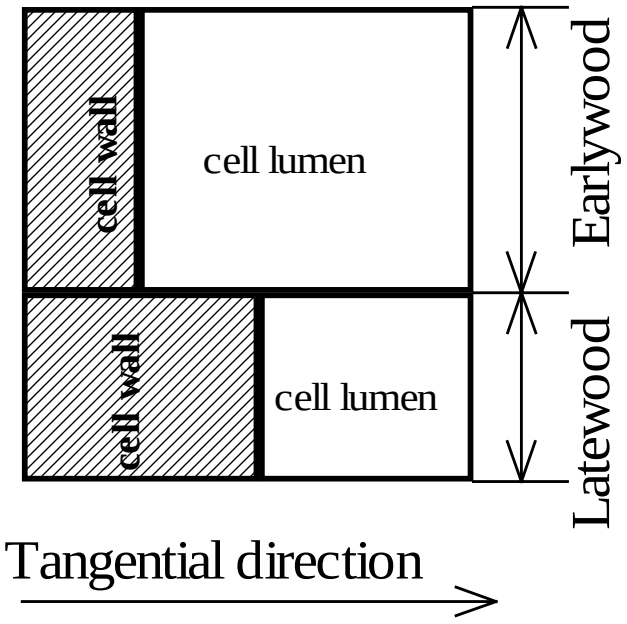

Figure 2. 10 Tangential geometric model for softwood species with MC below FSP

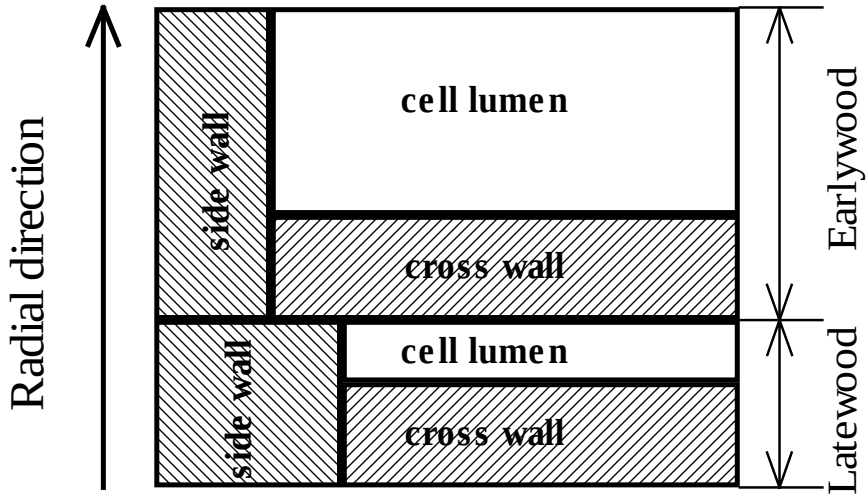

Figure 2. 11 Radial geometric model for softwood species with MC below FSP.

These two geometrical models were for the dry sample or the samples with moisture content (MC) below the fiber saturation point (FSP, usually 30%MC). Fiber saturation point is the special moisture content point at which wood contains no liquid water in the cell cavities but fully saturated cell walls with bound water attached to the hydrogen-bonding sites. An example illustration of the moisture change in a single cell is shown in Figure 2.22. There are 3 states for water existing in wood: bound water, water vapor and free water. When wood is under ovendry condition, there is no moisture at all in wood. Below FSP, moisture in wood exists as bound water in the cell walls and vapors in the cell lumens. FSP is when bound water are taken all the possible hydrogen-bonding sites in the cell wall and the lumen are full of saturated water vapor, but no free water in the lumen. When MC is over the FSP, some free water will appear in the lumens. The amount of free water in the lumen depends on the total MC of wood. When the lumen is filled up with all the free water, the fully saturation state of wood is reached. At this state, wood has the maximum MC. When free water takes part of the cell lumens, there will be significant change in the estimated effective thermal conductivity in both directions because water has much greater thermal conductivity value than air and vapor. Since the arrangement of free water and vapor in the cell lumen is hard to model due to the surface tension between free water and vapor, a mixture of free water and vapor is assumed to be exist in the cell lumen. The weighed average of the free water thermal conductivity and vapor conductivity values in the

lumen is used in the geometric models for the MC over the FSP. Geometric models for wet softwood samples (with MC above the FSP) are the same as the ones for MC below FSP, only replacing the pure vapor thermal conductivity by the weight average thermal conductivity in the cell lumen for the models above FSP.

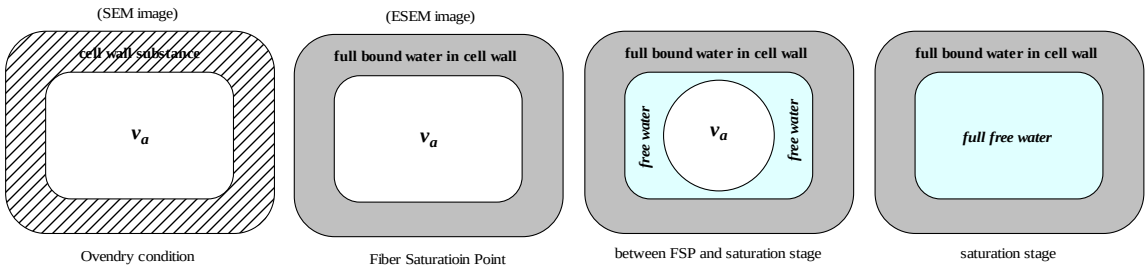

Figure 2. 12 Single cell structure change from dry to fully saturated condition.

The percentage of air and/or vapor in the cell lumen can be calculated based on Siau's (1995) wood porosity (V_a) definition:

$$V_a = 1 - G(\frac{1}{G_0^w} + 0.01MC)$$

Equa. (2. 1)

Where, G ---- specific gravity;

G_0^w ---- ovendry cell wall specific gravity, =1.53;

MC ---- moisture content (%);

V_a is calculated based on total volume V of wood. According to Gong (1992), in order base it on the volume of cell lumen, it needs to be multiplied by V/V_{lumen}, which is the inverse of V_a at MC=0. So,

$$V_1 = \frac{1 - G(\frac{1}{G_0^w} + 0.01MC)}{1 - G\frac{1}{G_0^w}}$$

Equa. (2. 2)

This V_1 is the percentage of porosity (contains air and vapor) in the cell lumen at certain MC above FSP. The fraction for the free water in the lumen will be:

$$V_{fw} = 1 - V_1$$

Equa. (2. 3)

The weighed average of thermal conductivity for vapor and free water in the cell lumen can be calculated as:

$$k_{aw} = V1 * k_a + (1 - V1) * k_w$$

Equa. (2. 4)

2.4.1.2 Geometric model for hardwoods

The structure of hardwoods is more heterogeneous without regular shaped cells. The cell wall substance and air/vapor in the lumens arranged alternately in both radial and tangential directions. The earlywood and latewood arrangement in the two directions is the same as the softwoods. One gross structure, which is different from the softwoods, is the considerable ray volume on the cross section. The ray percentage for soft maple on the cross section was measured to be about 15% to 18%. Since the ray cells run in the radial direction on the horizontal plane, which is perpendicular to the axis of the other cells, it has to be a separate part shown in the geometric models (Figure 2.25 and 2.26). The latewood portion in soft maple is small and less varied based on visual observation of many samples, and the percentage for the latewood in maple samples is measured to be about 15% to 20%. Therefore the percentage of latewood in the model for estimating soft maple thermal conductivities was assumed to be a constant percentage as a value of 20%. This will be used as the input in the later model calculations of soft maple thermal conductivities.

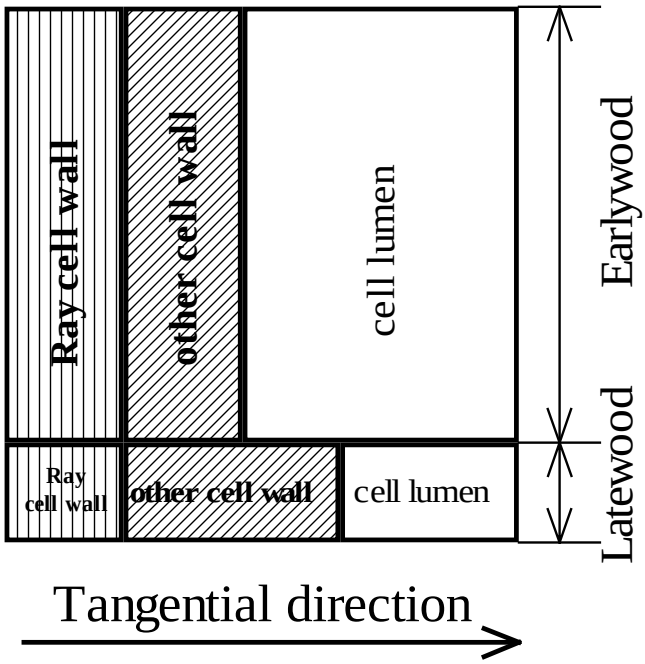

Figure 2. 13 Tangential geometric model for hardwood species with MC below FSP

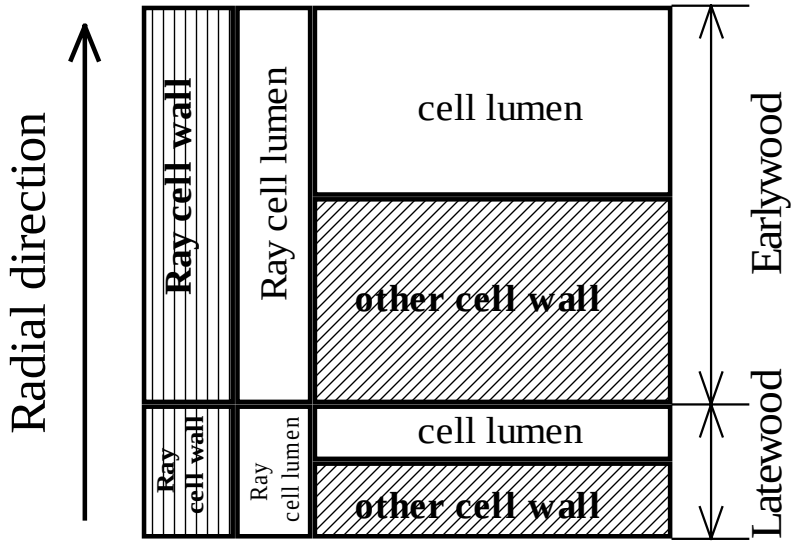

Figure 2. 14 Radial geometric model for hardwood species with MC below FSP.

2.4.2 Theoretical derivation of thermal conductivity

2.4.2.1 Derivation of thermal conductivity for softwood species

2.4.2.1.1 Thermal resistance model

The analogous electrical resistance system can be applied here in order to derive the overall thermal conductivity as a resultant value from the known thermal conductivities of its substances. The thermal resistance models for radial and tangential directions generated from the geometric models are shown in Figure 2.27. For MC above the FSP, thermal resistance models are the same due to the same geometric models. But the resistance from the air will be replaced by the resistance from the mixture of air and free water in the cell lumen.

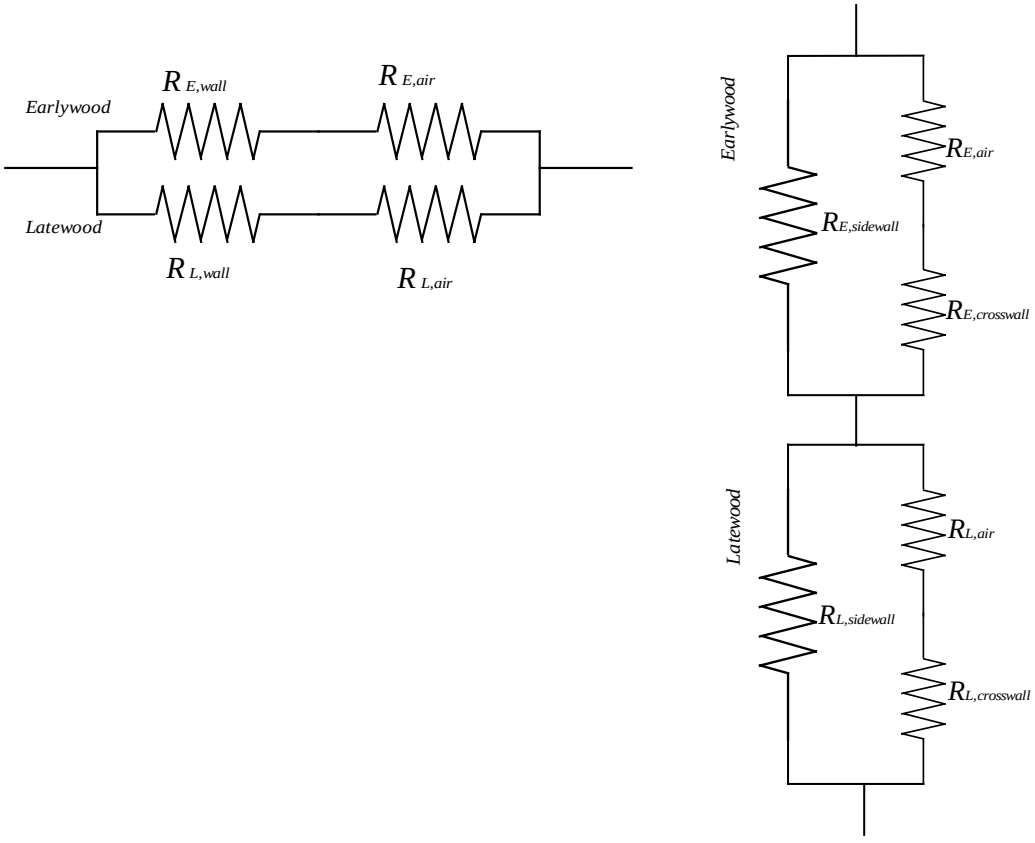

Figure 2. 15 Thermal resistance model for softwood species tangential (left) and radial (right) direction when MC is below FSP.

Introducing the electrical conductance definition into the thermal system gives the thermal conductance defined as:

$$g = k\frac{A}{L}$$

Equa. (2. 5)

Where, g ---- thermal conductance, W/K;

k ---- thermal conductivity, W/m·K;

A ---- cross section of the heat flow, m^2;

L ---- length of the heat flow, m;

Thermal resistance (R) is the inverse of the thermal conductance:

$$R = \frac{1}{g} = \frac{L}{kA}$$

Equa. (2. 6)

2.4.2.1.2 *Tangential thermal conductivity derivation*

According to the electrical resistance calculation in parallel or series systems, the effective thermal conductivity in tangential direction is obtained by:

$$\frac{1}{R_{T,eff}} = \frac{1}{R_E} + \frac{1}{R_L}$$

Equa. (2. 7)

Where, $R_{T,eff.}$ ---- total effective thermal resistance in tangential direction;

R_E ---- total thermal resistance from the earlywood part;

R_L ---- total thermal resistance from the latewood part;

Equation (2.25) is based on the parallel arrangement of the earlywood and latewood in the tangential direction. Within the earlywood or latewood area, cell wall substance and air in the lumens are arranged in series. So,

$$R_E = R_{E,wall} + R_{E,air}$$
$$R_L = R_{L,wall} + R_{L,air}$$

Equa. (2. 8)

Where, $R_{E,wall}$ ---- resistance from earlywood cell wall substance;

$R_{E,air}$ ---- resistance from the air in earlywood cell lumen;

$R_{L,wall}$ ---- resistance from latewood cell wall substance;

$R_{L,air}$ ---- resistance from the air in latewood cell lumen;

By the definition and anatomical measurement results, each of these resistances can be calculated by:

$$R_{E,wall} = \frac{TED\% * L}{k_c * E\% * A};$$
$$R_{E,air} = \frac{(1 - TED\%) * L}{k_a * E\% * A};$$

$$R_{L,wall} = \frac{TLD\% * L}{k_c * L\% * A};$$
$$R_{L,air} = \frac{(1 - TLD\%) * L}{k_a * L\% * A}$$

$$R_{T,eff} = \frac{L}{k_{T,eff} * A}$$

Where, *TED%* ---- cell wall percentage in *T*angential direction of *E*arlywood *D*ry sample;

E% ---- *E*arlywood percentage measured in wood samples;

TLD% ---- cell wall percentage in *T*angential direction of *L*atewood *D*ry sample;

L% ---- *L*atewood percentage measured in wood samples;

By plugging all these resistances into the *Equation 2.26*, *Equation 2.25* and *Equation 2.24*, the effective tangential thermal conductivity for the dry softwood samples can be calculated. The detailed calculation is implemented in *Mathematica* software for the easy operation and convenient replications. All the percentage parameters required in the calculation were obtained from the anatomical test. The thermal conductivity values for cell wall substance and air in the lumen were taken from Maku (1954):

$k_{c,\perp}$ = 0.41 W/m·K;

k_a = 0.046 W/m·K;;

For the wet sample model (MC above FSP), the thermal resistance in cell lumen is assumed to be from the mixture of vapor and free water for both earlywood and latewood in the tangential direction. The total thermal resistance in the tangential direction is calculated by the same as the above with only the thermal resistance from cell lumen are calculated for the mixture as shown below. And the cell wall percentages in earlywood and latewood are also different from the ovendry models and calculations.

$$R_{E,wall} = \frac{TEW\% * L}{k_c * E\% * A};$$
$$R_{E,airwater} = \frac{(1 - TEW\%) * L}{k_{aw} * E\% * A};$$

$$R_{L,wall} = \frac{TLW\% * L}{k_c * L\% * A};$$
$$R_{L,airwater} = \frac{(1 - TLW\%) * L}{k_{aw} * L\% * A};$$

Where, *TEW%* ---- cell wall percentage in *T*angential direction of *E*arlywood *W*et sample;

TLW% ---- cell wall percentage in *T*angential direction of *L*atewood *W*et sample;

k_{aw} ---- thermal conductivity of the mixture, calculated from *Equation (2.23)*;

The thermal conductivity for pure water is:

k_{water} = 0.59 W/m·K; (Siau 1995)

The numerical results calculated from *Mathematica* software will be shown in the next section.

2.4.2.1.3 *Radial thermal conductivity derivation*

With the series arrangement of earlywood and latewood in the radial direction (see Figure 2.21 and Figure 2.27 right), the total effective thermal resistance in the radial direction is:

$$R_{R,eff} = R_E + R_L$$

Equa. (2. 9)

Where, $R_{R,eff.}$ ---- the total effective thermal resistance in radial direction;

Within each earlywood or latewood area, the thermal resistance arrangement is more complicated than in the tangential direction (Figure 2.20 and 2.21).Part of the cell walls (side walls) are arranged in parallel with the series arrangement of the other part of cell wall (cross walls) and air in cell lumen. So the resistances from earlywood and latewood are:

$$\frac{1}{R_E} = \frac{1}{R_{E,sidewall}} + \frac{1}{R_{E,air} + R_{E,crosswall}}$$
$$\frac{1}{R_L} = \frac{1}{R_{L,sidewall}} + \frac{1}{R_{L,air} + R_{L,crosswall}}$$

Equa. (2. 10)

Where, $R_{E,sidewall}$ ---- resistance from earlywood side walls;

$R_{E,air}$ ---- resistance from air in earlywood cell lumens;

$R_{E,crosswall}$ ---- resistance from earlywood cross walls;

$R_{L,sidewall}$ ---- resistance from latewood side walls;

$R_{L,air}$ ---- resistance from air in latewood cell lumens;

$R_{L,crosswall}$ ---- resistance from latewood cross walls;

By definition and anatomical measurement results, each of these resistances can be calculated:

$$R_{E,sidewall} = \frac{E\% * L}{k_c * RESD\% * A};$$
$$R_{E,air} = \frac{E\% * (1 - RECD\%) * L}{k_a * (1 - RESD\%) * A};$$
$$R_{E,crosswall} = \frac{E\% * RECD\% * L}{k_c * (1 - RESD\%) * A};$$

$$R_{L,sidewall} = \frac{L\% * L}{k_c * RLSD\% * A};$$
$$R_{E,air} = \frac{L\% * (1 - RLCD\%) * L}{k_a * (1 - RLSD\%) * A};$$
$$R_{E,crosswall} = \frac{L\% * RLCD\% * L}{k_a * (1 - RLSD\%) * A};$$

$$R_{R,eff} = \frac{L}{k_{R,eff} * A}$$

Where, *RESD%* ---- *S*ide wall percentage in *E*arlywood *R*adial direction of *D*ry sample;

RECD% ---- *C*ross wall percentage in *E*arlywood *R*adial direction of *D*ry sample;

RLSD% ---- *S*ide wall percentage in *L*atewood *R*adial direction of *D*ry sample;

RLCD% ---- *C*ross wall percentage in *Late*wood *R*adial direction of *D*ry sample;

All these parameters were obtained from the anatomical tests in the previous section. By plugging these resistance into *Equation 2.27* and *Equation 2.28*, the effective radial thermal conductivity for the dry softwood samples can be calculated.

Thermal resistance model in the radial direction for wet wood samples (MC above FSP) is the same as the one for MC below FSP. Therefore the derivation is the same, except with the thermal resistance from cell lumen is calculated for the mixture of vapor and water instead of single pure vapor. Total thermal resistance in the radial direction is still calculated as *Equation*

2.27. The resistance from earlywood (R_E) and latewood (R_L) are different with the mixture thermal resistance replacing the vapor resistance:

$$\frac{1}{R_E} = \frac{1}{R_{E,sidewall}} + \frac{1}{R_{E,airwater} + R_{E,crosswall}}$$
$$\frac{1}{R_L} = \frac{1}{R_{L,sidewall}} + \frac{1}{R_{L,airwater} + R_{L,crosswall}}$$

Where the individual resistance are calculated based on the percentages measured from the wet samples:

$$R_{E,sidewall} = \frac{E\% * L}{k_c * RESW\% * A};$$
$$R_{E,airwater} = \frac{E\% * (1 - RECW\%) * L}{k_{aw} * (1 - RESW\%) * A};$$
$$R_{E,crosswall} = \frac{E\% * RECW\% * L}{k_c * (1 - RESW\%) * A};$$

$$R_{L,sidewall} = \frac{L\% * L}{k_c * RLSW\% * A};$$
$$R_{L,airwater} = \frac{L\% * (1 - RLCW\%) * L}{k_{aw} * (1 - RLSW\%) * A};$$
$$R_{L,crosswall} = \frac{L\% * RLCW\% * L}{k_c * (1 - RLSW\%) * A};;$$

Where, *RESW%* ---- *S*ide wall percentage in *E*arlywood *R*adial direction for *W*et sample;

RECW% ---- *C*ross wall percentage in *E*arlywood *R*adial direction for *W*et sample;

RLSW% ---- *S*ide wall percentage in *L*atewood *R*adial direction for *W*et sample;

RLCW% ---- *C*ross wall percentage in *Late*wood *R*adial direction for *W*et sample;

k_{aw} ---- thermal conductivity of the vapor and free water mixture (calculated from *Equation (2.23)*);

All the calculation and results are shown in the following section.

2.4.2.2 Derivation of thermal conductivity of hardwood species

2.4.2.2.1 Thermal resistance model

The thermal resistance models for the hardwood species were given in Figure 2.29 based on the geometric models of hardwoods (Figure 2.25and Figure 2.26). The total resistance from earlywood and latewood are in parallel system for the tangential direction, but in series systems for the radial direction. This is the same as softwood models. The only difference is the ray part in both the radial and tangential hardwood models which was not seen in the softwood models. In the tangential direction, the ray cells are arranged in series with all the other longitudinal cells wall substances and lumens. While in the radial direction, rays are in parallel with those cells wall substances and lumens. Based on soft maple geometric models, the thermal resistance models in the radial and tangential directions can be set up as:

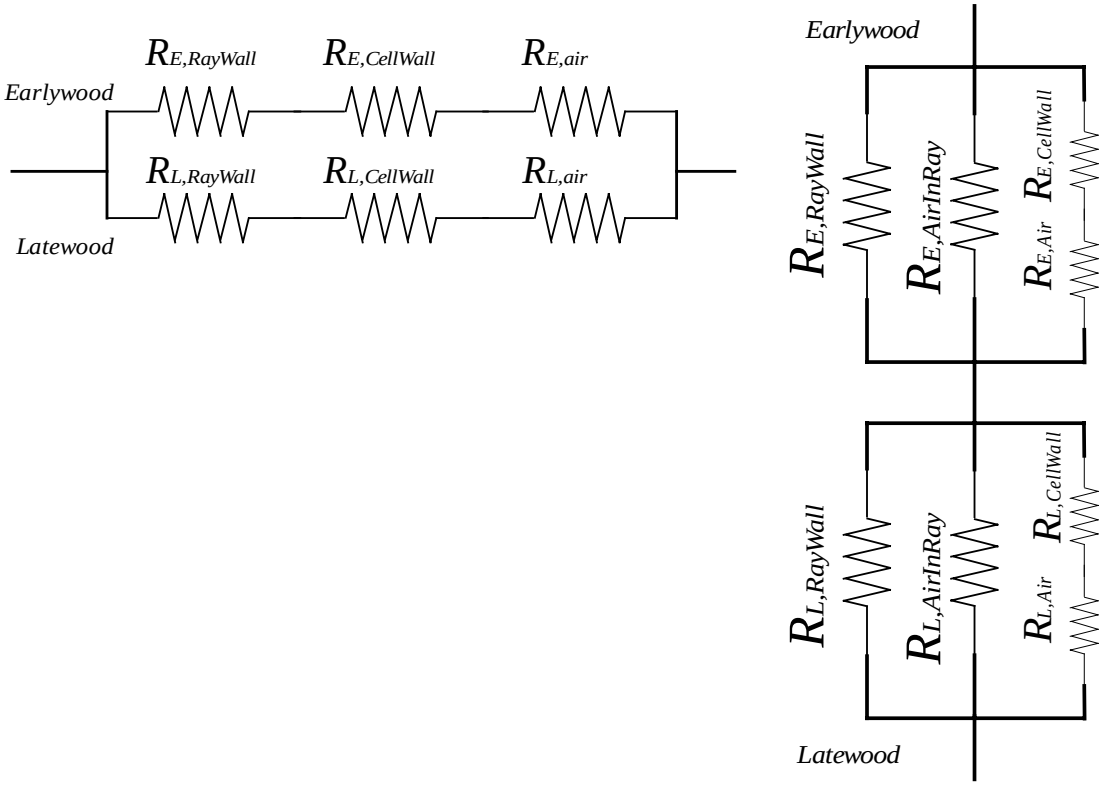

Figure 2. 16 Thermal resistance model for hardwood species tangential (left) and radial (right) direction when MC is below FSP.

2.4.2.2.2 Tangential thermal conductivity derivation

For the parallel arrangement of earlywood and latewood in the tangential direction, the total effective thermal resistance in the tangential direction is:

$$\frac{1}{R_{T,eff}} = \frac{1}{R_E} + \frac{1}{R_L}$$

Equa. (2. 11)

Within each earlywood or latewood, resistance from ray cell wall substance and air in ray cell lumen are in series with the resistance from other cell wall substance and air in lumens. So,

$$R_E = R_{E,RayWall} + R_{E,CellWall} + R_{E,air};$$
$$R_L = R_{L,RayWall} + R_{L,CellWall} + R_{L,air};$$

Equa. (2. 12)

Where, $R_{E,RayWall}$ ---- resistance from wall substance of the earlywood ray cells;

$R_{E,CellWall}$ ---- resistance from wall substance of other cells in the earlywood area;

$R_{E,air}$ ---- resistance from air in the cell lumens of the earlywood;

$R_{L,RayWall}$ ---- resistance from wall substance of the latewood ray cells;

$R_{L,CellWall}$ ---- resistance from wall substance of other cells in the latewood area;

$R_{L,air}$ ---- resistance from air in the cell lumens of the latewood;

Although the ray percent in earlywood and latewood area is the same because all the rays run through both earlywood and latewood, the resistances for the ray part from earlywood and latewood were separated here and below for convenience and clarification in the calculation. By definition and anatomical measurement results, each of these resistances can be defined as:

$$R_{E,CellWall} = \frac{(TE\% - Ray\%) * L}{k_{c,\perp} * E\% * A};$$

$$R_{E,air} = \frac{(1 - TE\%) * L}{k_a * E\% * A};$$

$$R_{E,RayWall} = \frac{Ray\% * L}{k_{c,//} * E\% * A};$$

$$R_{L,CellWall} = \frac{(TL\% - Ray\%) * L}{k_{c,\perp} * L\% * A};$$

$$R_{L,air} = \frac{(1 - TL\%) * L}{k_a * L\% * A};$$

$$R_{L,RayWall} = \frac{Ray\% * L}{k_{c,//} * L\% * A};$$

Where, *TE%* ---- total cell wall percentage in the *T*angential direction of *E*arlywood;

TL% ---- total cell wall percentage in the *T*angential direction of *L*atewood;

Ray% ---- ray percentage on the cross section;

It should be mentioned that the cell wall substance in the ray cells is parallel to their axis when seen on the cross section. So for heat transfer in the transverse direction, the thermal conductivity value for the ray cell wall substance should use the parallel value ($k_{c,//}$) instead of the vertical value ($k_{c,\perp}$) used for the other cell wall substance, which are perpendicular to the cell axes. The parallel-to-axis $k_{c,//}$ value is twice the perpendicular-to-axis value $k_{c,\perp}$, according to Siau (1995):

$k_{c,//}$ = 0.84 W/m.K

By plugging all the known values and percentage parameters obtained from the anatomical tests into *Equation 2.29* and *Equation 2.30*, the effective thermal conductivity for the tangential direction hardwood species can be estimated. The results will be shown in the "Numerical Results" section.

2.4.2.2.3 *Radial thermal conductivity derivation*

The existence of earlywood and latewood in the radial and tangential direction is the same for all the species, no matter softwoods or hardwoods. So the total effective thermal resistance of maple in the radial direction is the same as softwood species shown in *Equation 2.27*:

$$R_{R,eff} = R_E + R_L$$

Within earlywood or latewood area, the thermal resistance arrangement for hardwood species is different from softwoods (see Figure 2.28 and Figure 2.29). The wood ray cells arranged in parallel with the series arrangement of the other longitudinal cells wall substance and lumens in the radial direction. The total resistance from earlywood and latewood are, respectively, represented as:

$$\frac{1}{R_E} = \frac{1}{R_{E,RayWall}} + \frac{1}{R_{E,AirInRay}} + \frac{1}{R_{E,wall} + R_{E,air}};$$
$$\frac{1}{R_L} = \frac{1}{R_{L,RayWall}} + \frac{1}{R_{L,AirInRay}} + \frac{1}{R_{L,wall} + R_{L,air}};$$

Equa. (2. 13)

Where, $R_{E,AirInRay}$ ---- resistance from air in the ray voids of earlywood;

$R_{L,AirInRay}$ ---- resistance from air in the ray voids of latewood;

All the individual resistances in the above equations are calculated as:

$$R_{E.CellWall} = \frac{E\% * RE\% * L}{k_{c,\perp} * (1 - Ray\%) * A};$$
$$R_{E,air} = \frac{E\% * (1 - RE\%) * L}{k_a * (1 - Ray\%) * A};$$
$$R_{E,RayWall} = \frac{E\% * L}{k_{c,//} * Ray\% * 4/9 * A};$$
$$R_{E,AirInRay} = \frac{E\% * L}{k_a * Ray\% * 5/9 * A};$$

$$R_{L.CellWall} = \frac{L\% * RL\% * L}{k_{c,\perp} * (1 - Ray\%) * A};$$

$$R_{L,air} = \frac{L\% * (1 - RL\%) * L}{k_a * (1 - Ray\%) * A};$$

$$R_{L,RayWall} = \frac{L\% * L}{k_{c,//} * Ray\% * 4/9 * A};$$

$$R_{L,AirInRay} = \frac{L\% * L}{k_a * Ray\% * 5/9 * A};$$

The percentage of the cell wall in the radial direction (*RE%* and *RL%*)measured from the wood anatomical structure is different from the percentage measured in the tangential direction (*TE%* and *TL%*). But the same ray volume percent (*Ray%*) is used in this radial model as in the tangential model. The same wall substance thermal conductivity values ($k_{c,//}$) for the rays was used in the radial model. It should be mentioned here that the ray cell lumen is separated from other cell lumens because this part in the model is arranged differently from the other lumens (see the Figure 2.26). It is assumed that 4/9 of the total ray volume is the wall substance and the rest is ray void.(see in $R_{E,RayWall}$, $R_{E,AirInRay,}$, $R_{L,RayWall}$, and $R_{L,AirInRay}$). This is for the simplification of the program.

The calculations were performed in *Mathematica*. The results are presented in the following section.

2.4.3 Numerical results for the model estimation

Mathematica is a very powerful software for large and complicated calculations and programming. Many built-in solvers, easy debugging and value estimation, clear layout and nice report designs make *Mathematica* the choice for solving the thermal conductivity models developed above. It will be used again for the two dimensional heat transfer model in the next chapter. As an example shown in Figure 2.30 of the *Mathematica* environment, it gives a clear layout of the program if the details are not necessary for the readers. Readers can choose to see the details of certain parts that they are interested in by clicking on the right bracket of those sections. For example, if readers care about the input and result plots, they can click on the brackets at the right side of these sections to display the details, and leave the Numerical Calculation section folded as it is. Another advantage for running in *Mathematica* is that it is easy

to find the parameters and change the values for repeated estimation. The speed of running estimation is also pretty fast.

The whole *Mathematica* program for calculation of the thermal conductivity models derived from the theory above are presented in the Appendix B.

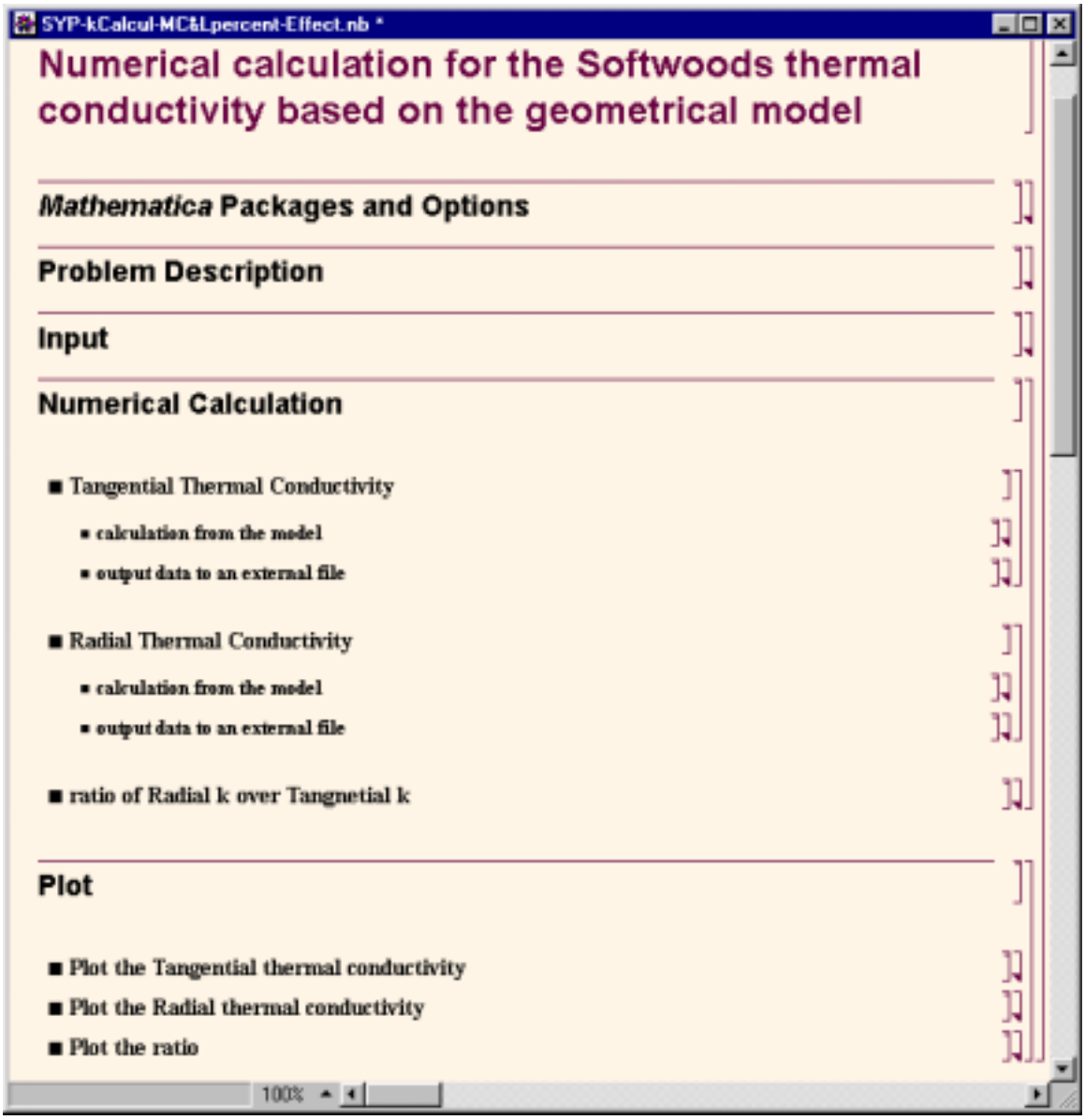

Figure 2. 17 Display of *Mathematica* software environment with the general clear layout of one program

2.4.3.1 Estimation results for southern yellow pine

The model estimation for southern yellow pine thermal conductivity in the two directions was based on the resistance models and derivations shown before. The equations were put into the calculation section. The input section gives the known constant parameters as shown below:

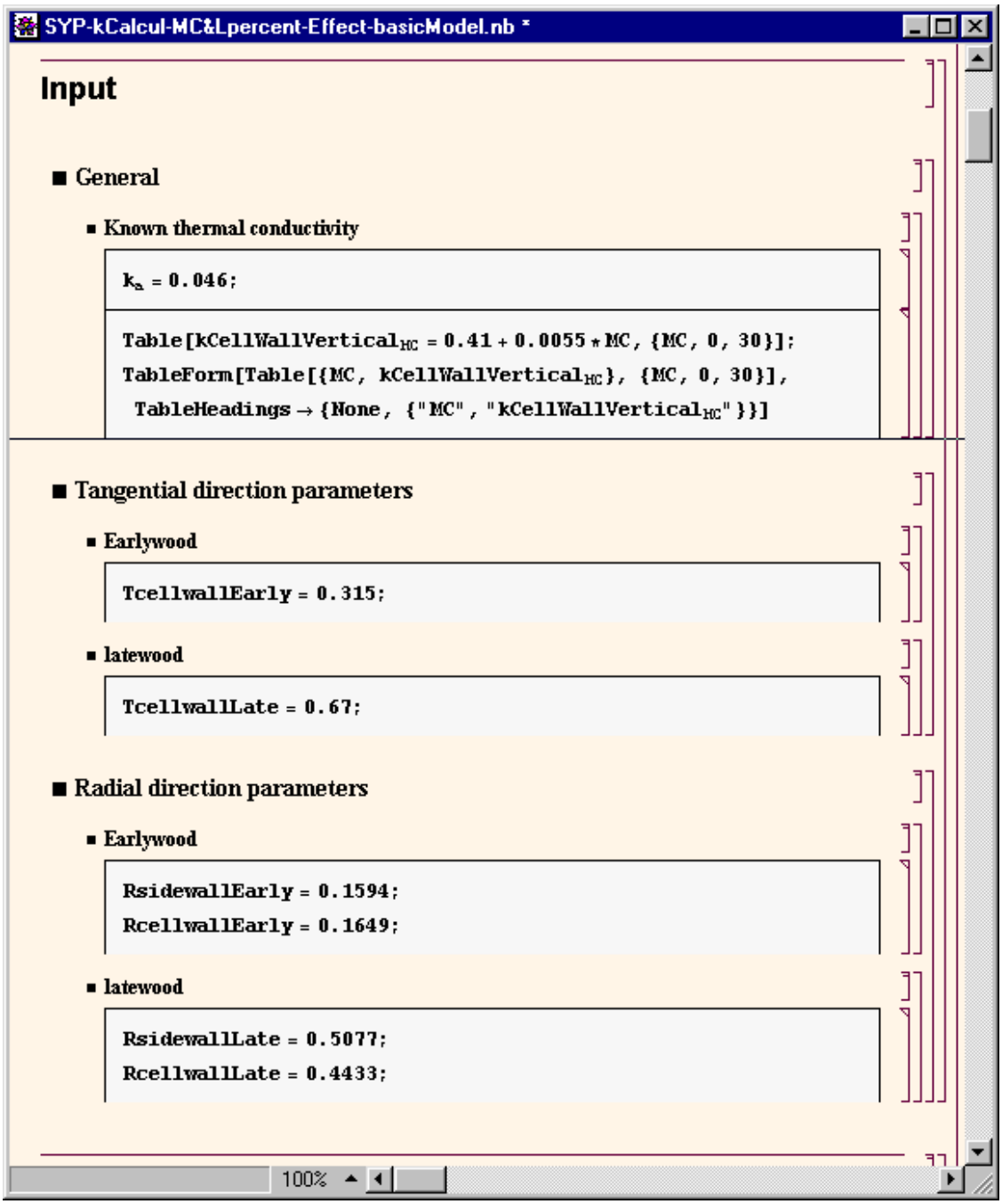

Figure 2. 18 The input section of southern yellow pine thermal conductivity model estimation model.

In this section, all the anatomical structure parameters were set as constant known parameters except for the earlywood and latewood percentage. Since the latewood (or earlywood) percent on the cross section may vary from sample to sample, this program set the latewood % (LW%) as a changing factor, ranging from 1% to 99%, and the program output a table of thermal conductivity values based on the different LW%. Although it may not be realistic for the latewood to be as very low (1%-10%) or very high (80%-99%) on the real wood samples, the response of the estimated thermal conductivity values as the change of latewood percent in the wide range is interesting to examine. The thermal conductivity value for air (k_a) in the lumen is set as the constant in the "General" subsection under the input section (see in Figure 2.31), while the thermal conductivity value for the cell wall substance k_c is defined as a function of moisture content based on the relationship given by Siau (1995):

$$k_{qT} = G(0.2 + 0.0038 * MC) + 0.024 \qquad [W/m \cdot K] \qquad for\ MC < 40\%$$

Equa. (2. 14)

where, k_{qT} ---- the transverse thermal conductivity;

G ---- specific gravity;

If k_c =0.41 W/m.K is the assumed value (Maku 1954) at the oven dry condition (MC=0%), and the specific gravity of the cell wall at the oven dry condition is 1.45 (Kellogg & Wangaard 1969), then the k_c as a function of MC can be approved to be:

$$k_c = 0.41 + 0.0055 * MC \qquad for\ MC \le 30\%$$

Equa. (2. 15)

This relation was used in the program shown above. k_c values were calculated from *0%* to *30%MC* in order to predict thermal conductivity changes for moisture contents under the FSP. Fiber Saturation Point was chosen to be the upper limit in this program because the geometric model and thermal resistance model will be different if the MC is over FSP due to the presence of free water.

The program gave estimation for thermal conductivity values of southern yellow pine for the latewood range from 1% to 99% and moisture content range from 0% to 30%. Part of the results is shown below in *Table 2.4* and *Table 2.5*. The full tables for all the estimated values in

the whole ranges can be found in Appendix A Table A-34 and Table A-35. The two-dimensional plots for the radial and tangential thermal conductivity changes with MC and latewood percent in the sample heat flow direction of samples are shown in Figure 2.29 and 2.30.

It can be seen from the tables that there is difference for model-predicted thermal conductivity values in the radial and tangential directions. Radial thermal conductivity is higher than the tangential values. Tangential model predicted thermal conductivities do not change significantly with the moisture content, while radial thermal conductivities change much more with moisture. Both radial and tangential thermal conductivities change with the latewood percentage on the cross section. Again radial is changing more than tangential thermal conductivity. From the model prediction, latewood volume in the sample has a substantial affect on the transverse thermal conductivity and heat transfer. This is consistent with previous literature results. It has been known for a long time that thermal conductivity is a positive linear function of specific gravity, and latewood percentage has a very close relationship with the specific gravity. The more the thick-cell-walled latewood in the samples, the higher the specific gravity.

Table 2. 4 Southern yellow pine model predicted tangential thermal conductivity values in the range of latewood percentage from 10% to 99% and MC from 0% to 30%.

Latewood percentage	Moisture content									
	0%	5%	10%	11%	12%	13%	14%	15%	20%	30%
10%	0.0688	0.0691	0.0694	0.0695	0.0695	0.0696	0.0696	0.0697	0.0699	0.0703
20%	0.0738	0.0742	0.0746	0.0747	0.0747	0.0748	0.0749	0.0749	0.0753	0.0758
30%	0.0788	0.0793	0.0798	0.0799	0.0800	0.0801	0.0801	0.0802	0.0806	0.0813
40%	0.0837	0.0844	0.0850	0.0851	0.0852	0.0853	0.0854	0.0855	0.0860	0.0868
45%	0.0862	0.0869	0.0876	0.0877	0.0878	0.0879	0.0880	0.0881	0.0887	0.0896
50%	0.0887	0.0895	0.0902	0.0903	0.0904	0.0905	0.0907	0.0908	0.0913	0.0923
55%	0.0912	0.0920	0.0927	0.0929	0.0930	0.0932	0.0933	0.0934	0.0940	0.0951
60%	0.0937	0.0945	0.0953	0.0955	0.0956	0.0958	0.0959	0.0961	0.0967	0.0979
70%	0.0986	0.0996	0.1005	0.1007	0.1009	0.1010	0.1012	0.1013	0.1021	0.1034
80%	0.1036	0.1047	0.1057	0.1059	0.1061	0.1063	0.1064	0.1066	0.1074	0.1089
90%	0.1086	0.1098	0.1109	0.1111	0.1113	0.1115	0.1117	0.1119	0.1128	0.1144
99%	0.1130	0.1144	0.1156	0.1158	0.1160	0.1162	0.1164	0.1166	0.1176	0.1194

Table 2. 5 Southern yellow pine model predicted radial thermal conductivity values in the range of latewood percentage from 10% to 99% and MC from 0% to 30%.

Latewood percentage	Moisture content									
	0%	5%	10%	11%	12%	13%	14%	15%	20%	30%
10%	0.1171	0.1219	0.1267	0.1276	0.1286	0.1295	0.1305	0.1315	0.1362	0.1458
20%	0.1243	0.1295	0.1347	0.1358	0.1368	0.1378	0.1389	0.1399	0.1451	0.1554
30%	0.1325	0.1382	0.1439	0.1450	0.1461	0.1472	0.1484	0.1495	0.1552	0.1664
35%	0.1370	0.1430	0.1489	0.1501	0.1513	0.1525	0.1536	0.1548	0.1607	0.1725
40%	0.1418	0.1481	0.1543	0.1556	0.1568	0.1580	0.1593	0.1605	0.1667	0.1791
45%	0.1470	0.1536	0.1601	0.1614	0.1628	0.1641	0.1654	0.1667	0.1732	0.1862
50%	0.1525	0.1595	0.1664	0.1678	0.1692	0.1706	0.1719	0.1733	0.1802	0.1939
55%	0.1586	0.1659	0.1732	0.1747	0.1761	0.1776	0.1790	0.1805	0.1878	0.2022
60%	0.1650	0.1728	0.1806	0.1821	0.1837	0.1852	0.1868	0.1883	0.1960	0.2113
70%	0.1798	0.1886	0.1974	0.1991	0.2009	0.2026	0.2044	0.2061	0.2149	0.2322
80%	0.1974	0.2075	0.2176	0.2196	0.2217	0.2237	0.2257	0.2277	0.2377	0.2577
90%	0.2188	0.2307	0.2425	0.2449	0.2472	0.2496	0.2519	0.2543	0.2660	0.2895
99%	0.2425	0.2564	0.2703	0.2731	0.2758	0.2786	0.2814	0.2841	0.2980	0.3256

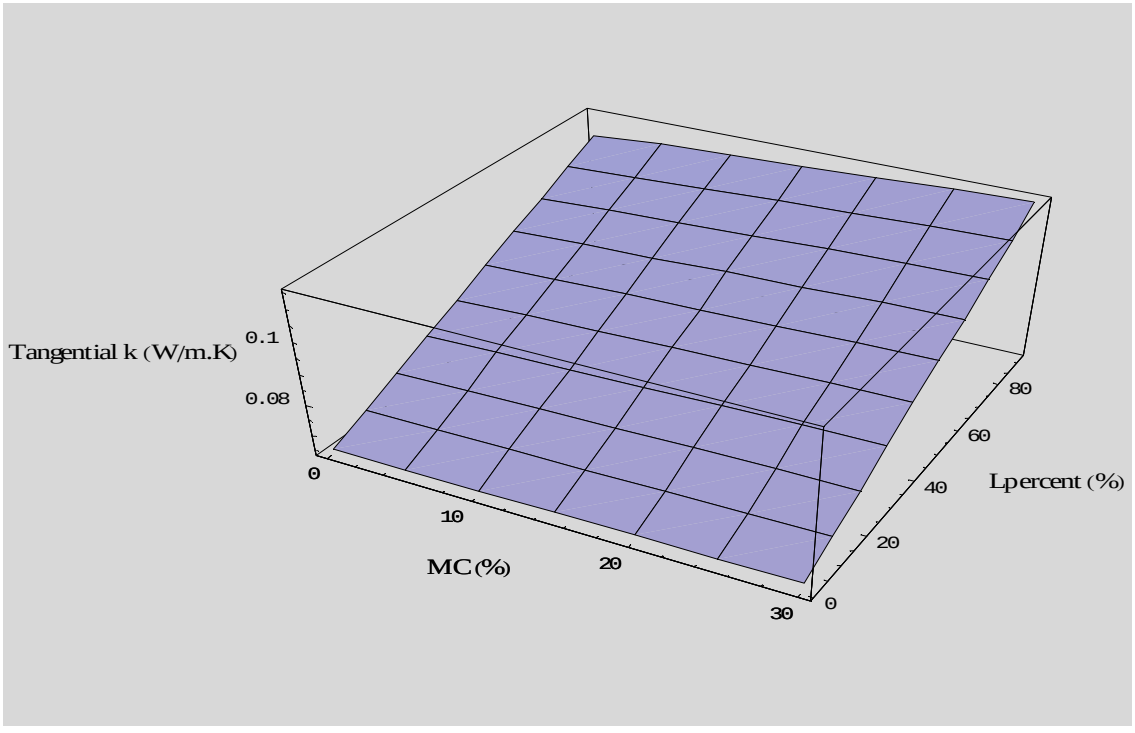

Figure 2. 19 Southern yellow pine model predicted tangential thermal conductivity values change with the latewood percentage on the cross section and moisture content change in the sample.

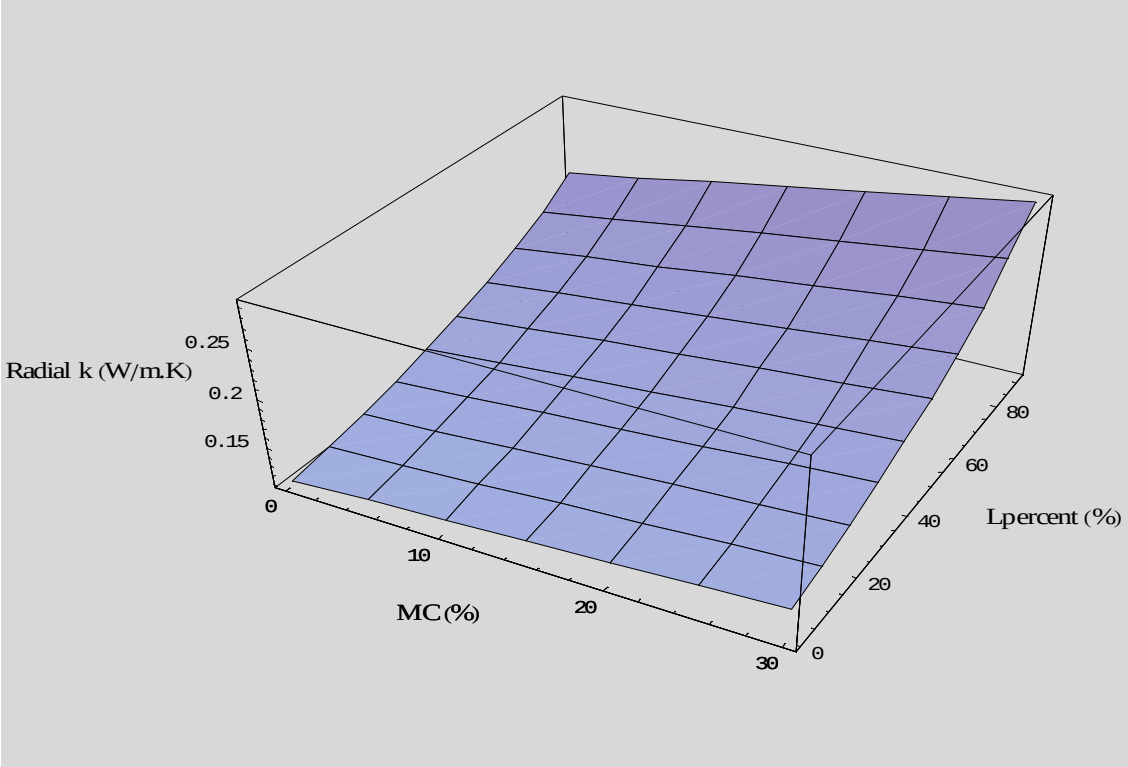

Figure 2. 20 **Southern yellow pine model predicted radial thermal conductivity values change with the latewood percentage on the cross section and moisture content in the sample.**

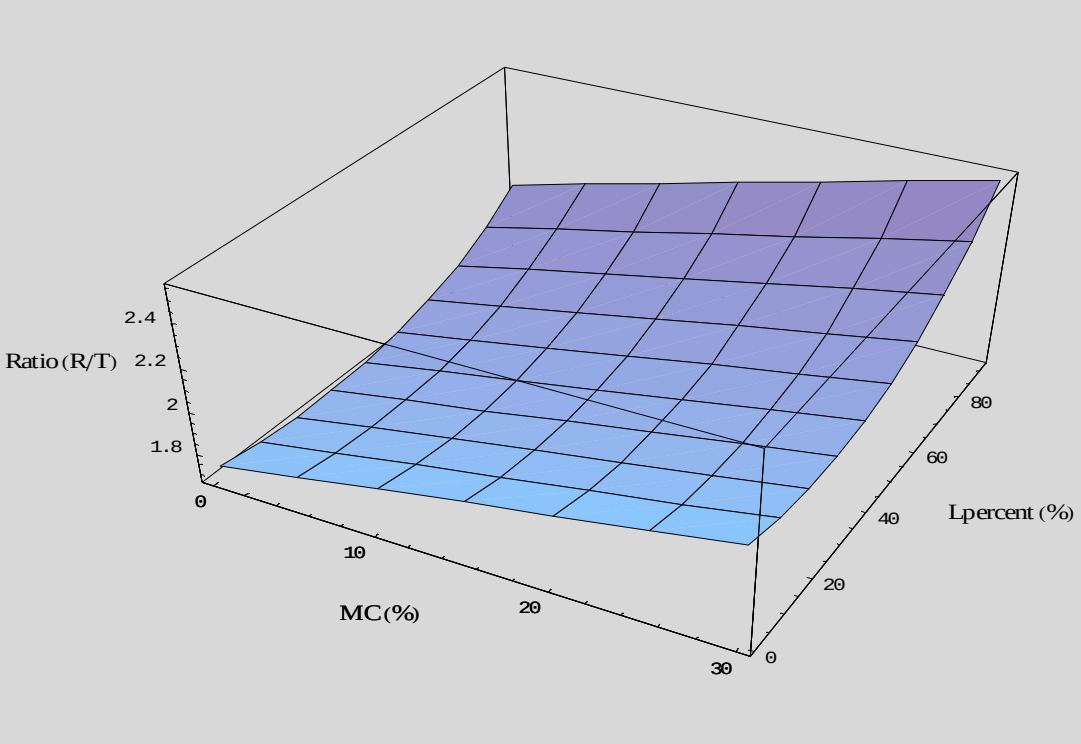

Figure 2. 21 **Southern yellow pine model predicted ratio of radial vs. tangential thermal conductivity with the change of latewood percentage on the cross section and moisture content in the sample.**

From the figures shown above, the radial and tangential thermal conductivity changes with moisture content (MC) and latewood (LW) percentage on the cross section of wood samples can be more clearly visualized. Tangential thermal conductivity (TTC) of southern yellow pine is predicted to change linearly with LW percent, but insignificantly changed with MC in the samples. Radial thermal conductivity (RTC) changes linearly with moisture content, and non-linearly with LW percentage. RTC is an inverse function of earlywood percentage (earlywood%=1-latewood%), which gives the trend as the lower the earlywood percentage (higher latewood percentage), the higher the RTC, and the increase of RTC is greater with the decrease of earlywood percentage (corresponding to the increase of latewood percentage). The ratio for RTC over TTC is basically controlled by the RTC because RTC is much greater and changes more significantly than TTC. The ratio ranges from 1.2 to 2.5 for the whole range shown.

In order to see only MC or only LW percent affect on the two thermal conductivities of southern yellow pine, a fixed LW percentage, such as, 30% LW, or a fixed MC, such as 10%MC, is chosen to be plotted. The plots are shown in Figures 2.32 and Figure 2.33. Insignificant change for TTC with MC and a linear change for TTC with LW percentage of southern yellow pine was found. MC affect on TTC is through the MC's affect on the k_c value (thermal conductivity of cell wall substance). TTC has little effect from the k_c value based on the examination of the mathematical derivation process described in last section. In the derivation, it showed that TTC is a linear function of LW percent. From practical sample point of view, it is also expected an increase of tangential thermal conductivity with the increase of latewood percentage in the sample. While the value change of cell wall substance thermal conductivity is expected to affect little on the general effective thermal conductivity value in the tangential direction due to another less-thermal-conducted component (air in the cell lumen) parallel arranged with the cell wall.

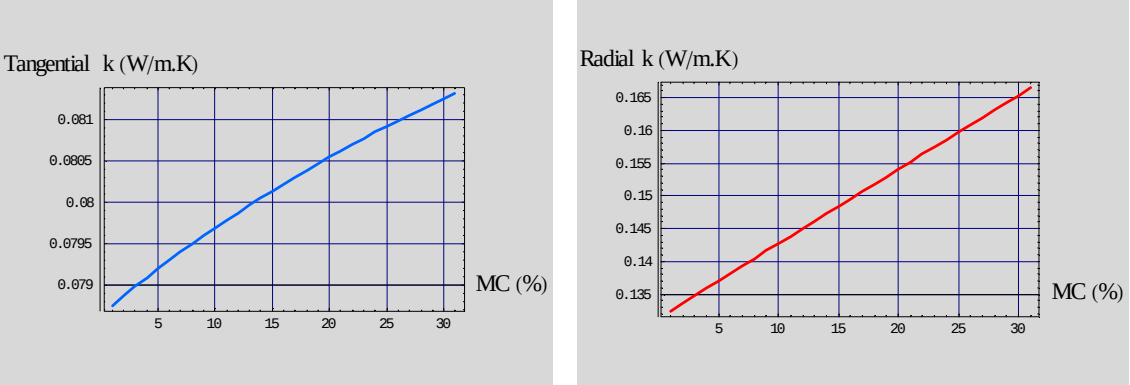

Figure 2. 22 An example plot for the tangential (left) and radial (right) thermal conductivity change as a function of the MC (from 0% to 30%) in a southern yellow pine sample with LW percent of 30%.

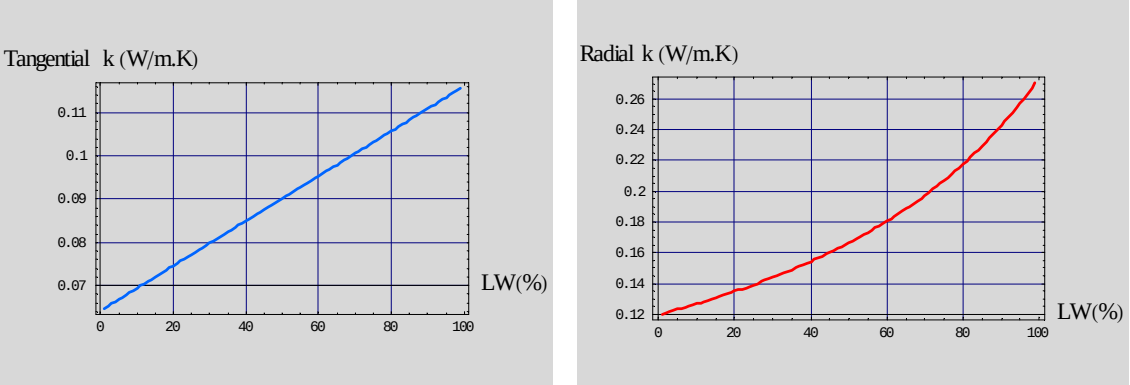

Figure 2. 23 An example plot for the tangential (left) and radial (right) thermal conductivity change as a function of the latewood percent (from 1% to 99%) in a southern yellow pine sample with MC of 10%.

A linear relation for the RTC with MC was found in the derivation and shown in Figure 2.32. The linear relationship comes from the side wall component effect in the geometric model, whose thermal conductivity value is a linear function of MC. An inverse relationship for RTC with (1-LW) percentage was found and shown in Figure 2.33. When LW percentage increase more and more, the effective thermal conductivity in the radial direction will increase more and more due to the series arrangement of the cross wall substance with the cell lumen in the radial direction and the separated side wall component parallel arranged in the geometric model.

2.4.3.2 Estimation results for Scots pine

2.4.3.2.1 Estimation from the model for the Scots pine sample below FSP

Scots pine sample with moisture content below FSP has the same geometric models and resistance models as southern yellow pine. So the same program was run for Scots pine model estimation for the two thermal conductivities in the *Mathematica*, and the same ranges (LW percentage from 1% to 99%, MC from 0% to 30%) were performed for the model outputs. The only change made in the program was the input parameters of the anatomical structures, such as cell wall percentage in earlywood radial direction and in earlywood tangential direction, etc. These parameters were shown not statistically different in the "Experimental Research…" section 2.3.2. So the model outputs for Scots pine thermal conductivities are almost the same as the ones for southern yellow pine part of the model outputs are shown in the *Table 2.6*, *Table 2.7*. The complete model outputs are shown in Appendix A, Table A-36 and A-37. Figure 2.37 to 2.41 gave visualized display for the change of thermal conductivity as functions of latewood percentage and MC in wood samples.

Table 2. 6 Scots pine model predicted tangential thermal conductivity values in the range of latewood percentage from 10% to 99% and MC from 0% to 30%.

Latewood percent	Moisture content (%)									
	0%	5%	10%	11%	12%	13%	14%	15%	20%	30%
10%	0.0700	0.0704	0.0707	0.0708	0.0708	0.0709	0.0709	0.0710	0.0713	0.0717
20%	0.0763	0.0768	0.0772	0.0773	0.0774	0.0775	0.0776	0.0776	0.0780	0.0787
30%	0.0825	0.0831	0.0837	0.0839	0.0840	0.0841	0.0842	0.0843	0.0848	0.0857
35%	0.0856	0.0863	0.0870	0.0871	0.0873	0.0874	0.0875	0.0876	0.0882	0.0891
40%	0.0887	0.0895	0.0903	0.0904	0.0905	0.0907	0.0908	0.0909	0.0915	0.0926
45%	0.0918	0.0927	0.0935	0.0937	0.0938	0.0940	0.0941	0.0943	0.0949	0.0961
50%	0.0949	0.0959	0.0968	0.0969	0.0971	0.0973	0.0974	0.0976	0.0983	0.0996
55%	0.0980	0.0991	0.1000	0.1002	0.1004	0.1006	0.1007	0.1009	0.1017	0.1031
60%	0.1011	0.1023	0.1033	0.1035	0.1037	0.1039	0.1040	0.1042	0.1051	0.1066
70%	0.1073	0.1086	0.1098	0.1100	0.1102	0.1105	0.1107	0.1109	0.1118	0.1135
80%	0.1136	0.1150	0.1163	0.1166	0.1168	0.1170	0.1173	0.1175	0.1186	0.1205
90%	0.1198	0.1214	0.1228	0.1231	0.1234	0.1236	0.1239	0.1242	0.1254	0.1275
99%	0.1254	0.1271	0.1287	0.1290	0.1293	0.1296	0.1299	0.1301	0.1314	0.1338

Table 2. 7 Scots pine model predicted radial thermal conductivity values in the range of latewood percentage from 10% to 99% and MC from 0% to 30%.

Latewood percent	Moisture content (%)									
	0%	5%	10%	11%	12%	13%	14%	15%	20%	30%
10%	0.1071	0.1111	0.1152	0.1160	0.1169	0.1177	0.1185	0.1193	0.1234	0.1315
20%	0.1143	0.1188	0.1233	0.1242	0.1251	0.1260	0.1268	0.1277	0.1322	0.1410
30%	0.1227	0.1276	0.1325	0.1335	0.1345	0.1355	0.1365	0.1374	0.1423	0.1521
35%	0.1274	0.1325	0.1377	0.1388	0.1398	0.1408	0.1418	0.1429	0.1480	0.1583
40%	0.1324	0.1379	0.1433	0.1444	0.1455	0.1466	0.1477	0.1488	0.1542	0.1650
45%	0.1378	0.1436	0.1494	0.1505	0.1517	0.1528	0.1540	0.1551	0.1609	0.1723
50%	0.1437	0.1499	0.1560	0.1572	0.1584	0.1597	0.1609	0.1621	0.1682	0.1803
55%	0.1501	0.1567	0.1632	0.1645	0.1658	0.1671	0.1684	0.1697	0.1762	0.1891
60%	0.1571	0.1642	0.1711	0.1725	0.1739	0.1753	0.1767	0.1781	0.1850	0.1987
70%	0.1734	0.1815	0.1895	0.1911	0.1927	0.1943	0.1959	0.1975	0.2055	0.2214
80%	0.1933	0.2028	0.2123	0.2142	0.2161	0.2180	0.2199	0.2218	0.2312	0.2499
90%	0.2184	0.2299	0.2414	0.2437	0.2459	0.2482	0.2505	0.2528	0.2641	0.2867
99%	0.2474	0.2614	0.2753	0.2781	0.2808	0.2836	0.2864	0.2892	0.3030	0.3307

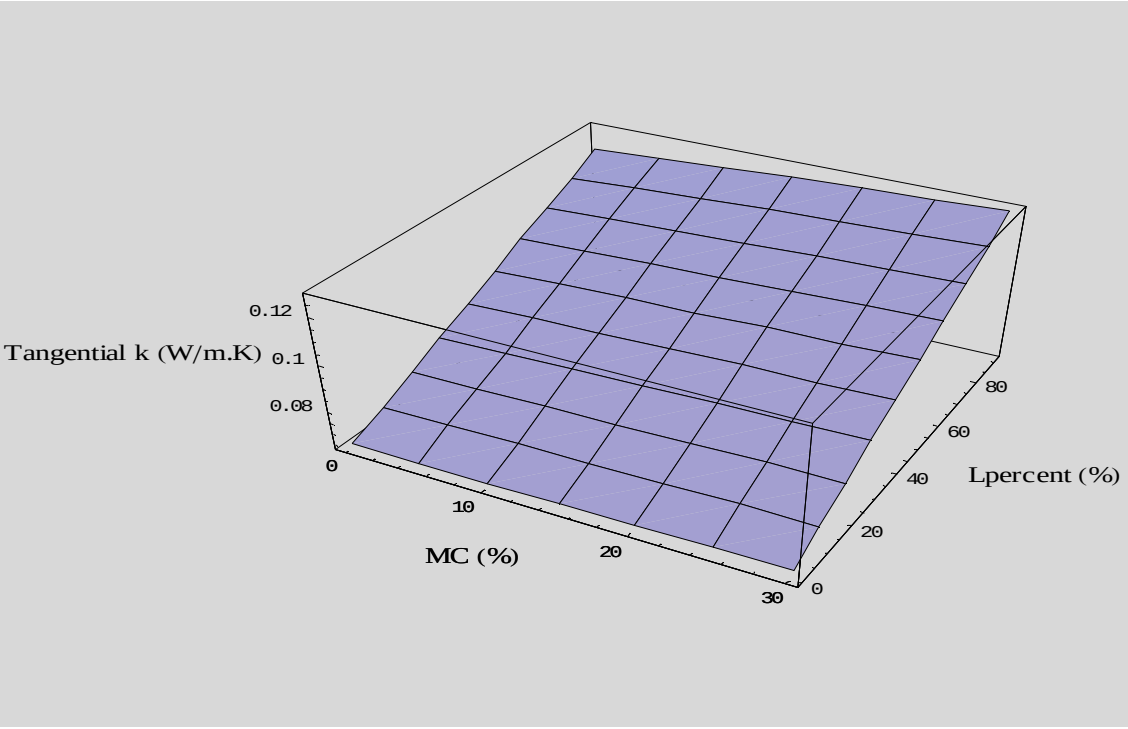

Figure 2. 24 Scots pine model predicted tangential thermal conductivity values change with the latewood percentage on the cross section and moisture content change in the sample.

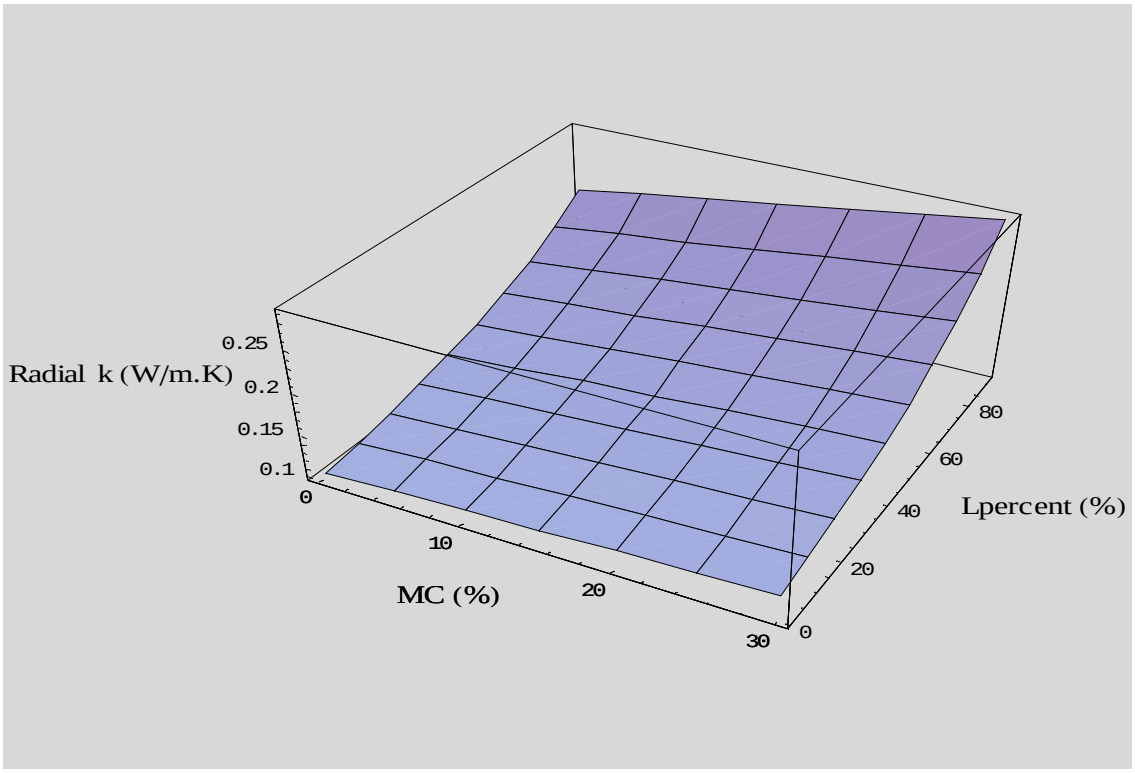

Figure 2. 25 **Scots pine model predicted radial thermal conductivity values change with the latewood percentage on the cross section and moisture content change in the sample.**

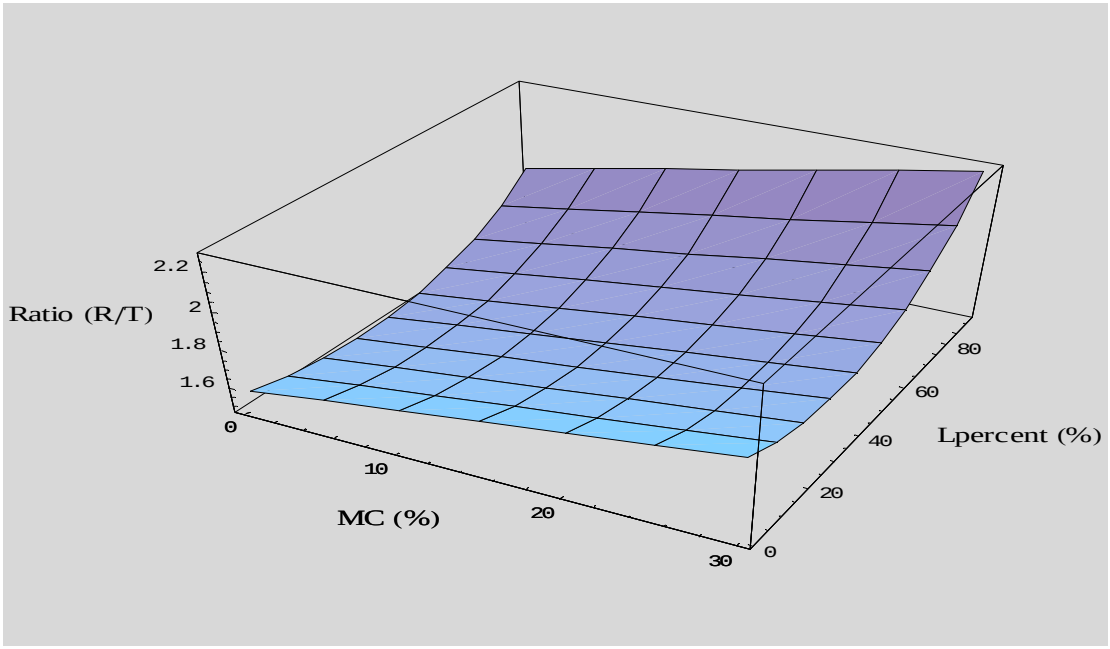

Figure 2. 26 **Scots pine model predicted ratio of radial vs. tangential thermal conductivity with the change of latewood percentage on the cross section and moisture content in the sample.**

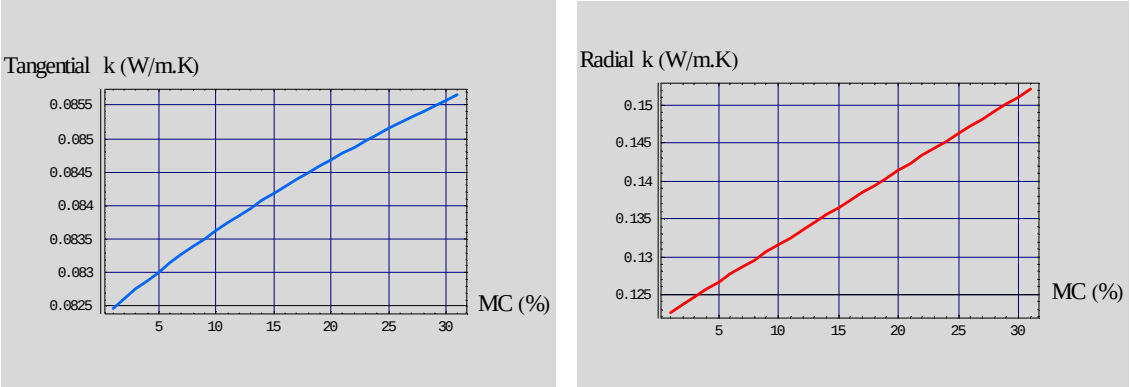

Figure 2. 27 An example plot for the tangential (left) and radial (right) thermal conductivity change only with the MC change (from 0% to 30%) for a Scots pine sample with LW percent of 30%.

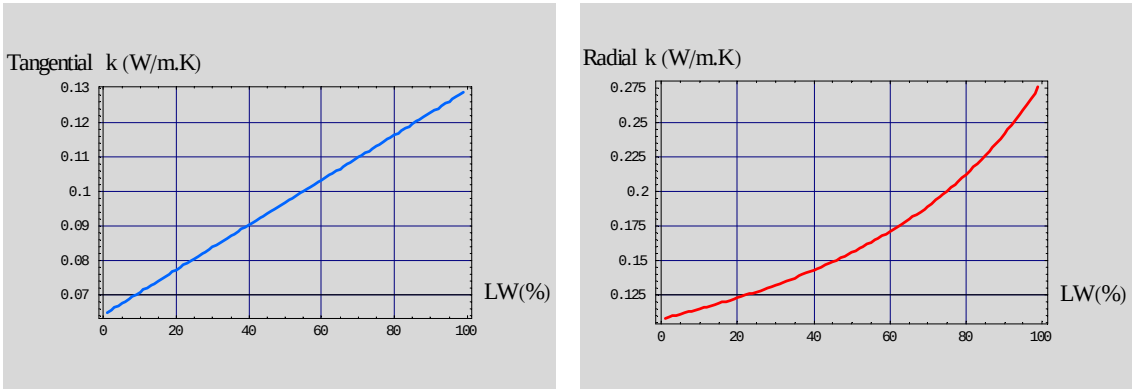

Figure 2. 28 An example plot for the tangential (left) and radial (right) thermal conductivity change with the latewood percent change (from 1% to 99%) for a Scots pine sample with MC of 10%.

2.4.3.2.2 Estimation from the model for the Scots pine sample above FSP

The geometric and thermal resistance models for softwood species, such as Scots pine, with MC above FSP are the same as the models for MC below FSP. The calculations of thermal conductivity in the two directions for the whole range of MC change will be performed in *Mathematica*, with first part for MC<30%, using pure vapor as the thermal resistance in the cell lumen, and second part for MC>30%, using the mixture of vapor and free water as the thermal resistance in the cell lumen. Before running the program, some more parameters or constants need to be defined. The anatomical structure parameters of wet samples obtained from ESEM images in the previous section are used.

The specific gravity for Scots pine samples with MC over the FSP and for the ovendry Scots pine samples were needed to calculate the V_1 -- the void in the cell lumens when there is certain amount of free water existing in the lumens. The specific gravity of wood is the ratio of the ovendry mass of wood to the mass of water displaced by the wood sample at a given moisture content. The increase of bound water in the cell wall causes swelling of the sample volume, which resulted in an increase of the mass of water displayed by the sample. So an increase of bound water in wood will decrease the specific gravity until the maximum swelling is reached, which is the FSP. Above the FSP, any increase of moisture will be in the free water state instead of bound water. Free water in the lumens does not change the dimension of wood samples. So wood has a maximum specific gravity value under ovendry condition (due to the minimum volume of the specimen) and has the minimum and constant value above the FSP. Two specific gravity values for red pine (*P.resinosa*), which is the similar species for Scots pine (*P. sylvestris*) according to Hoadley (1980), were found from Haygreen & Bowyer's textbook (1982):

$G_{green} = 0.48$ and

$G_{dry} = 0.41$

From ovendry condition to 30%MC, specific gravity is changing with the moisture content. But for simplification of program, only one G_{dry} value was used for MC below 30%. And G will be constant for MC above 30% with the value of G_{green}. The specific gravity for the cell wall has been given before with the value of 1.45 (Kellog & Wangaard 1969). The thermal conductivity of cell wall substance changes with moisture content below FSP was modified *(Equation 2.35)* based on MacLean's (1941) empirical equations. Above the FSP, cell wall substance stays the same with fully saturation of bound water. Therefore the thermal conductivity

of cell wall substance does not change above the FSP. The input parameters and relations can be seen clearly from the program input section shown below (Figure 2.39).

$$k_c = 0.41 + 0.0055 * MC \qquad [W/m \cdot K] \qquad for\ MC \le 30\%$$

Equa. (2. 16)

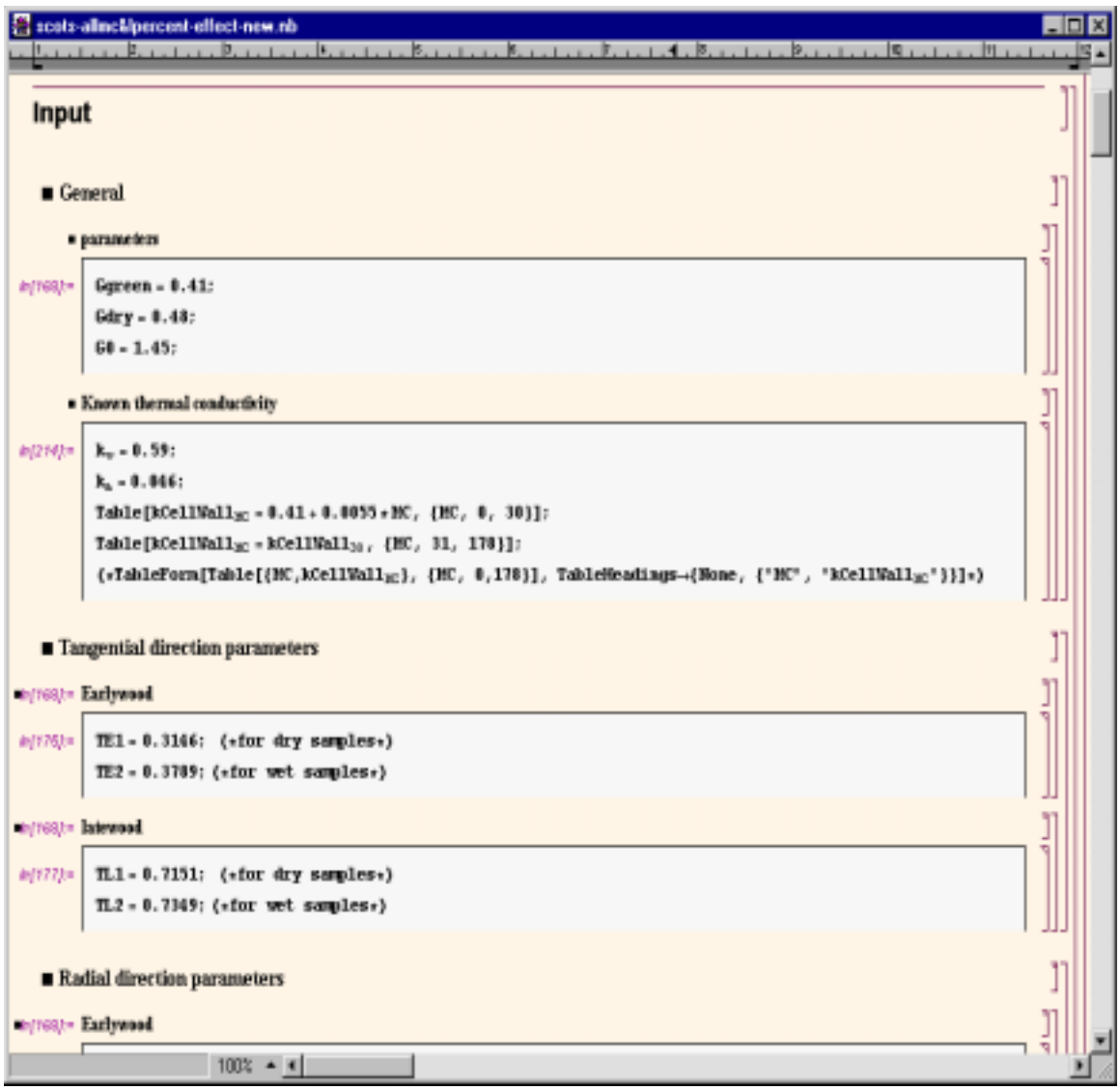

Figure 2. 29 The input parameters for the program to predict all the thermal conductivities of Scots pine in MC range from 0% to saturated.

The maximum moisture content that Scots pine can have under the fully saturated condition was calculated by the equation given by Siau (1995):

$$MC_{\max} = \frac{100}{G_{dry}} - 65.3$$

Equa. (2. 17)

The calculated result for MC_{max} of 178%, was used in the program (shown above in the input section) as the upper limit.

The model outputs are shown below, with tables giving the calculated data, and figures showing the trend for the thermal conductivity changes with the two factors. The full tables and complete data from the model estimations are shown in Appendix A, Table A-38 and A-39.

Table 2. 8 Scots pine model predicted tangential thermal conductivity values in the range of latewood percentage from 5% to 99% and MC from 0% to maximum 178%.

Latewood	Moisture content (%)											
percent	0%	5%	15%	30%	40%	60%	80%	100%	120%	140%	160%	178%
5%	0.0669	0.0672	0.0677	0.0682	0.2023	0.2789	0.3465	0.4066	0.4606	0.5093	0.5535	0.5900
10%	0.0700	0.0704	0.0710	0.0717	0.2083	0.2848	0.3516	0.4108	0.4636	0.5111	0.5541	0.5895
20%	0.0763	0.0768	0.0776	0.0787	0.2202	0.2966	0.3620	0.4192	0.4697	0.5148	0.5554	0.5886
30%	0.0825	0.0831	0.0843	0.0857	0.2321	0.3083	0.3724	0.4275	0.4757	0.5184	0.5566	0.5877
40%	0.0887	0.0895	0.0909	0.0926	0.2440	0.3201	0.3827	0.4359	0.4818	0.5221	0.5579	0.5868
50%	0.0949	0.0959	0.0976	0.0996	0.2559	0.3318	0.3931	0.4442	0.4879	0.5258	0.5591	0.5859
60%	0.1011	0.1023	0.1042	0.1066	0.2678	0.3436	0.4035	0.4526	0.4939	0.5294	0.5604	0.5850
70%	0.1073	0.1086	0.1109	0.1135	0.2797	0.3553	0.4138	0.4610	0.5000	0.5331	0.5616	0.5842
80%	0.1136	0.1150	0.1175	0.1205	0.2916	0.3671	0.4242	0.4693	0.5061	0.5368	0.5629	0.5833
90%	0.1198	0.1214	0.1242	0.1275	0.3035	0.3789	0.4346	0.4777	0.5121	0.5404	0.5641	0.5824
99%	0.1254	0.1271	0.1301	0.1338	0.3142	0.3894	0.4439	0.4852	0.5176	0.5437	0.5652	0.5816

Table 2. 9 Scots pine model predicted radial thermal conductivity values in the range of latewood percentage from 5% to 99% and MC from 0% to maximum 178%.

Latewood	Moisture content (%)											
percent	0%	5%	15%	30%	40%	60%	80%	100%	120%	140%	160%	178%
5%	0.1038	0.1077	0.1155	0.1272	0.2410	0.2998	0.3555	0.4084	0.4587	0.5065	0.5521	0.5913
10%	0.1071	0.1111	0.1193	0.1315	0.2464	0.3052	0.3605	0.4127	0.4620	0.5086	0.5528	0.5907
20%	0.1143	0.1188	0.1277	0.1410	0.2580	0.3166	0.3709	0.4215	0.4687	0.5129	0.5544	0.5895
30%	0.1227	0.1276	0.1374	0.1521	0.2707	0.3288	0.3819	0.4307	0.4756	0.5173	0.5559	0.5884
40%	0.1324	0.1379	0.1488	0.1650	0.2847	0.3420	0.3936	0.4403	0.4828	0.5217	0.5575	0.5873
50%	0.1437	0.1499	0.1621	0.1803	0.3003	0.3564	0.4060	0.4503	0.4902	0.5262	0.5590	0.5861
60%	0.1571	0.1642	0.1781	0.1987	0.3177	0.3720	0.4192	0.4608	0.4978	0.5308	0.5606	0.5850
70%	0.1734	0.1815	0.1975	0.2214	0.3372	0.3890	0.4333	0.4718	0.5056	0.5355	0.5622	0.5839
80%	0.1933	0.2028	0.2218	0.2499	0.3593	0.4076	0.4484	0.4834	0.5137	0.5403	0.5638	0.5827
90%	0.2184	0.2299	0.2528	0.2867	0.3844	0.4281	0.4646	0.4955	0.5220	0.5451	0.5654	0.5816
99%	0.2474	0.2614	0.2892	0.3307	0.4102	0.4485	0.4802	0.5069	0.5298	0.5496	0.5668	0.5806

From results shown in the table, we found that tangential thermal conductivity increases very significantly when free water appears in wood (MC>30%). And above the FSP, the moisture content shows much more affects on the tangential thermal conductivity than it does below the FSP. This is due to appearance of the high thermal-conducted free water in the lumens. Before the free water appears, air in the lumen has very low conductance, which contributes very little to the total effective conductance in the tangential direction (with series arrangement of the cell wall and cell lumen). The thermal conductivity of free water ($k_c=0.59$) is much higher than that of air, and even higher than thermal conductivity of cell wall substance. The appearance of free water in the lumen increases the total effective conductance in the tangential direction, and with its volume increase, the conductance will increase, too. Moisture content or free water appearance also has a same positive affect on the total effective conductance in the radial direction, too, but not as significant as the tangential direction. The increase tendency for both thermal conductivities is similar (as can be seen in the Figure 2.40 and Figure 2.41), with the tangential thermal conductivity increases more significantly than the radial one. The thermal conductivity increases nonlinearly with moisture content above the FSP in both radial and tangential directions. The thermal conductivities in the two directions were predicted to be close with the ratio near 1 for MC above FSP. For the fully saturated softwood samples, the transverse thermal conductivity is comparable to that of concrete ($k=0.93$) or glass ($k=1.05$) (Siau 1995).

The ratio of the two thermal conductivities predicted by the model in the whole range changed dramatically when MC reaches the FSP. Below the FSP, the ratio is tend to follow the radial thermal conductivity change because radial values and changes are much more significant than the tangential ones. At the 30% MC point, the ratio (R/T) dropped straight down to near 1.0, which means that the tangential thermal conductivity jumps close to the radial thermal conductivity when free water appears in the sample according to the model's prediction. The ratio (R/T) stays around 1.0 for the moisture content of samples reaches the saturated MC. So above the FSP, according to the model estimation, the thermal conductivities in the two directions are not significantly different from each other.

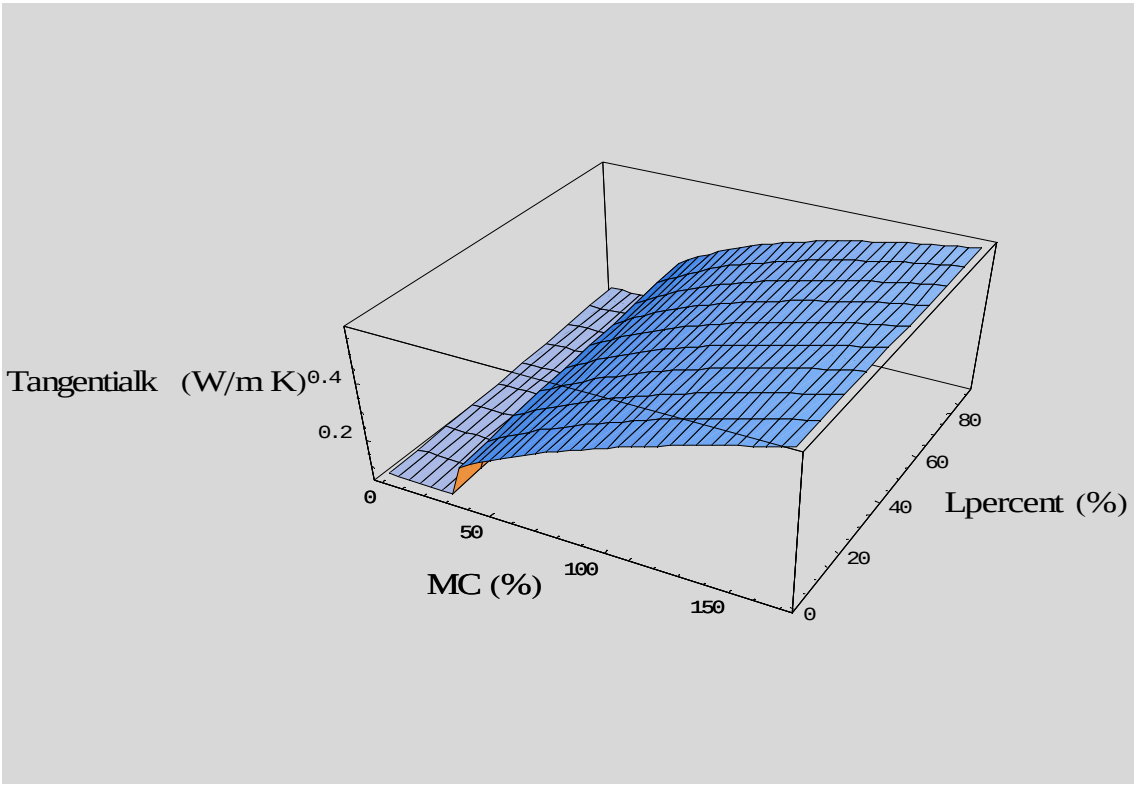

Figure 2. 30 **Scots pine model predicted tangential thermal conductivity values change with the latewood percentage on the cross section and moisture content change (the whole range) in the sample.**

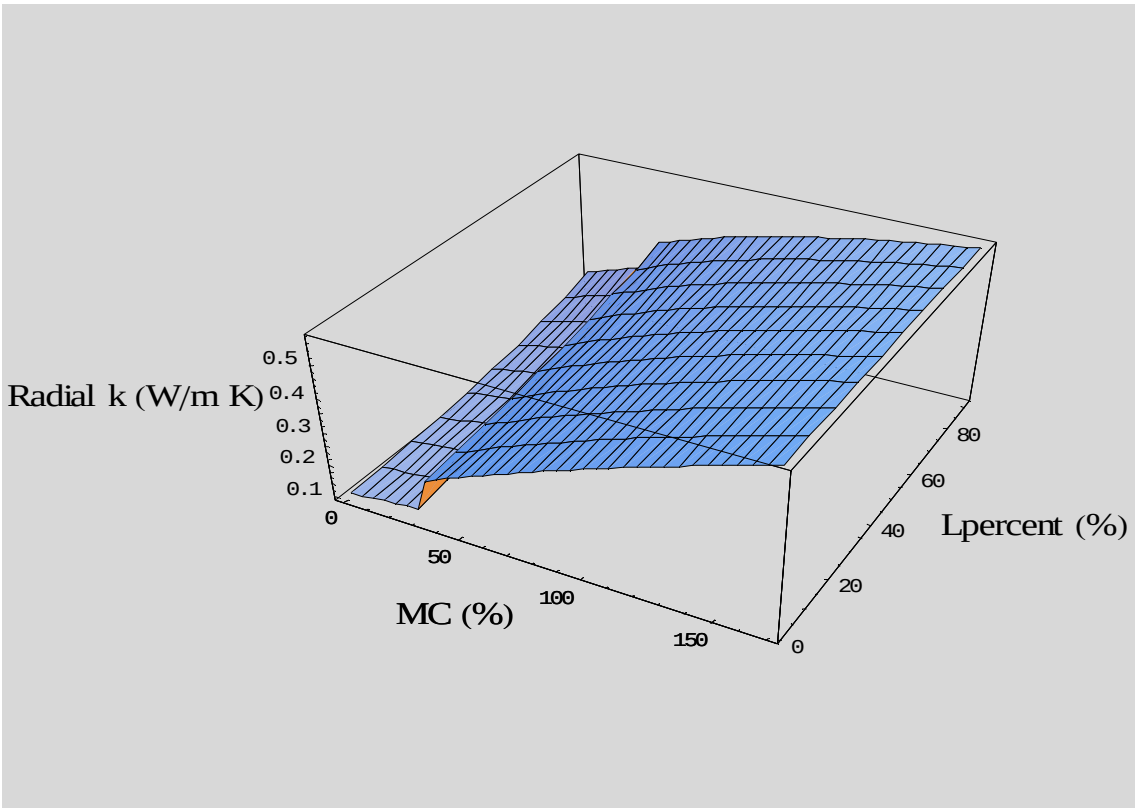

Figure 2. 31 **Scots pine model predicted radial thermal conductivity values change with the latewood percentage on the cross section and moisture content change (the whole range) in the sample.**

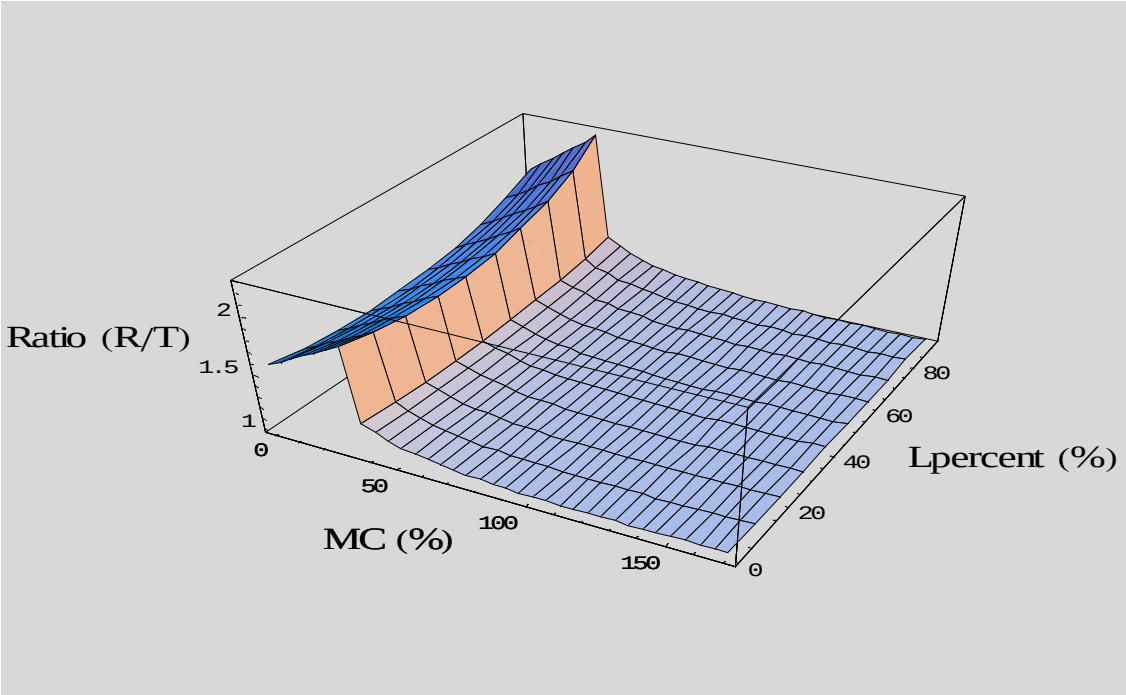

Figure 2. 32 Scots pine model predicted ratio of radial vs. tangential thermal conductivity with the change of latewood percentage on the cross section and moisture content (the whole range) in the sample.

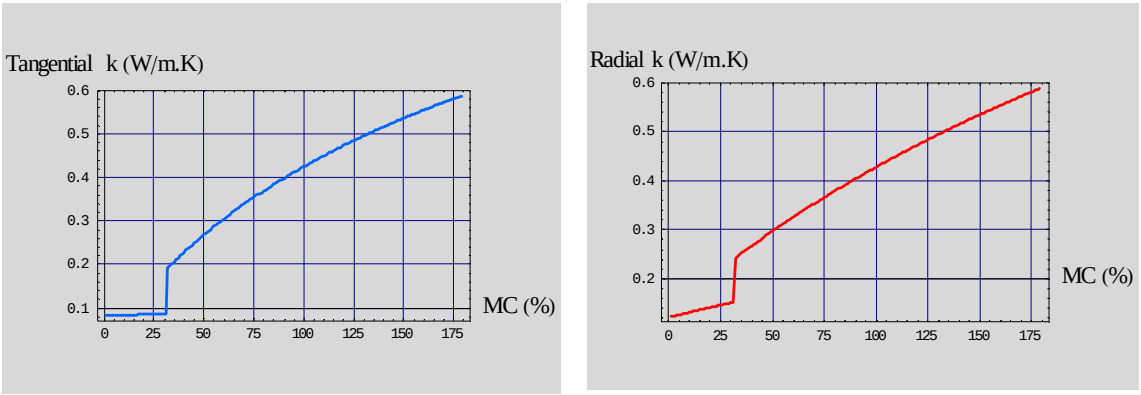

Figure 2. 33 Scots pine tangential and radial thermal conductivity change in the whole moisture range (from 0% to fully saturated) for a fixed latewood percent on the sample (LW=30%).

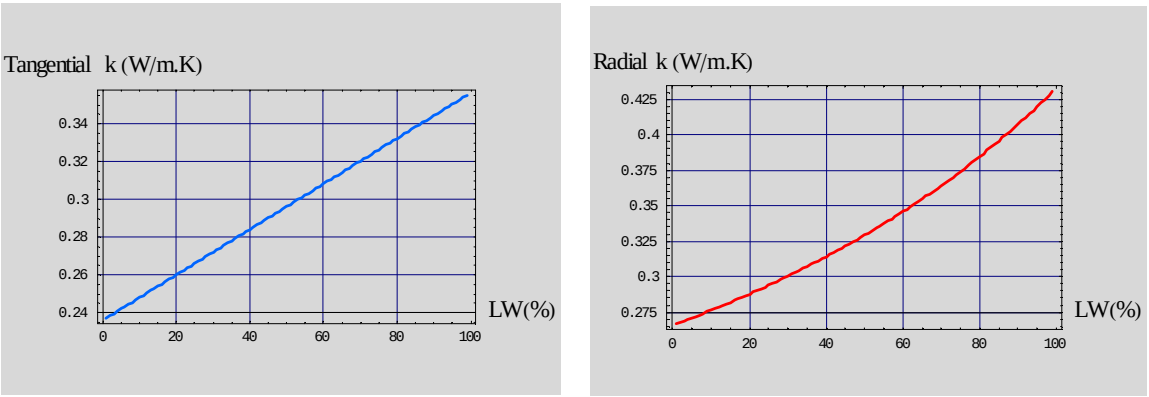

Figure 2. 34 Scots pine tangential and radial thermal conductivity change with latewood percent on the samples for a fixed moisture contend in the sample (MC=50%).

In order to observe the individual effect on the TTC and RTC from MC or LW percentage in the samples, TTC and RTC as a function of MC with LW% assumed of 30% are plotted in Figure 2.43, and TTC, RTC as a function of LW% with MC% assumed of 50% are plotted in Figure 2.44. It was found that moisture content over the FSP has a very powerful effect on both radial and tangential thermal conductivity. A significant jump for the TTC and RTC at MC reaches the FSP was found. When MC is over FSP (30% MC), a non-linear relationship is shown between the thermal conductivity and MC for both radial and tangential directions. The linear relationship between RTC and MC below the FSP was found before and is shown here in Figure 2.44. An insignificant relation between the TTC and MC was shown in Figure 2.43 when MC is below FSP. With the free water appearing in the cell lumens (MC over the FSP), the difference between the radial and tangential thermal conductivity is very small, which infers that the arrangement of earlywood and latewood in the two directions, and cell wall percentage and arrangement in the two directions become less affective on the resulted thermal conductivities than they did before the free water replacing the air in the cell lumen. The insulated property of wood is due to the less conducted air in the cell lumen. When free water takes part of the cell lumen, the structure difference in the two directions does not have significant effect on the resulted thermal conductivities in two directions. The effect from the LW percentage is the same for the MC below and above FSP on both radial and tangential thermal conductivity (Figure 2.44). Linear effect from the LW percentage on TTC and inverse effect from (1-LW%) on RTC is shown in Figure 2.44, too. RTC is slightly higher than TTC for the whole LW% range (1%-99%) in the samples with MC of 50%.

2.4.3.3 Estimation results for the hardwood species -- maple

The difference for the maple thermal conductivity model from the other two softwood species models is the ray structure included in the models. Total ray volume on the maple's cross section was measured to be about 18%. The ray cell wall substance lies perpendicular to the other cell wall substance due to the ray cells run in the radial direction on the transverse section. So the two parts of cell wall were separated in the models. The value of the thermal conductivity for the perpendicular cell wall substance changed in the same way with moisture content as described before. The thermal conductivity for the parallel cell wall substance is two times the perpendicular value according to Siau (1995).

$$k_{c,//} = 2 * k_{c,\perp};$$

Equa. (2. 18)

The input section of the model program for the maple thermal conductivity estimation is shown in Figure 2.45. An assumption of an estimated constant LW percentage of 20% was made because the latewood on maple cross section is not varied significantly from sample to sample due to its small amount. The percentage for LW was measured approximately between 10% to 20% in the previous section.

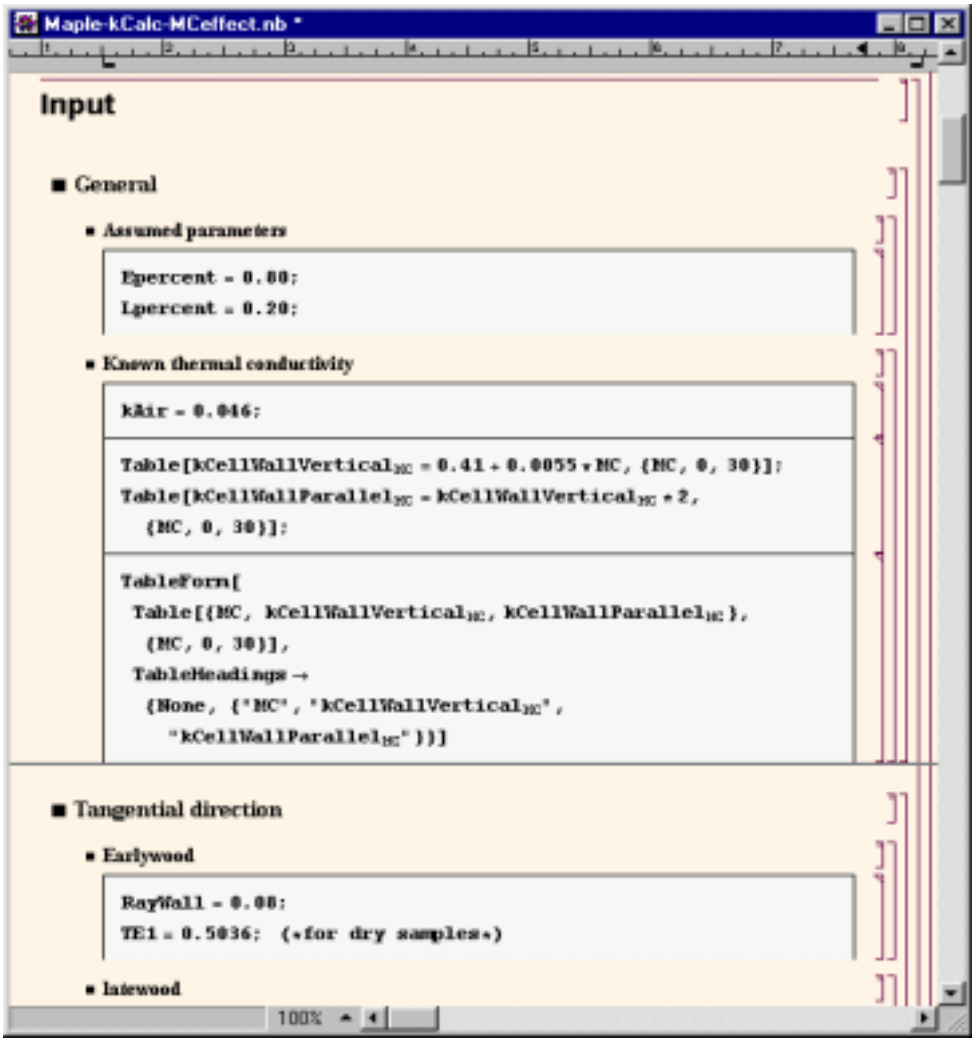

Figure 2. 35 The input parameters for the program to predict all the thermal conductivities of soft maple in MC range from 0% to 30%.

The model estimation for maple thermal conductivity in the radial and tangential direction in the range of MC from 0% to 30% is shown in the *Table 2.10*. The complete data of the model output for both directions are in the Appendix A, Table A-40. The plot for the two thermal conductivity changes with moisture content is shown in Figure 2.46.

Table 2. 10 Maple model predicted radial and tangential thermal conductivity values, and the ratios (R/T) in the MC change from 0% to maximum 30%.

Latewood	*MC (%)*	$K_{tangential}$	K_{radial}	*Ratio (R/T)*
20%	0%	0.0917	0.1300	1.42
	5%	0.0924	0.1347	1.46
	10%	0.0930	0.1394	1.50
	15%	0.0936	0.1440	1.54
	20%	0.0941	0.1486	1.58
	25%	0.0946	0.1532	1.62
	30%	0.0951	0.1578	1.66

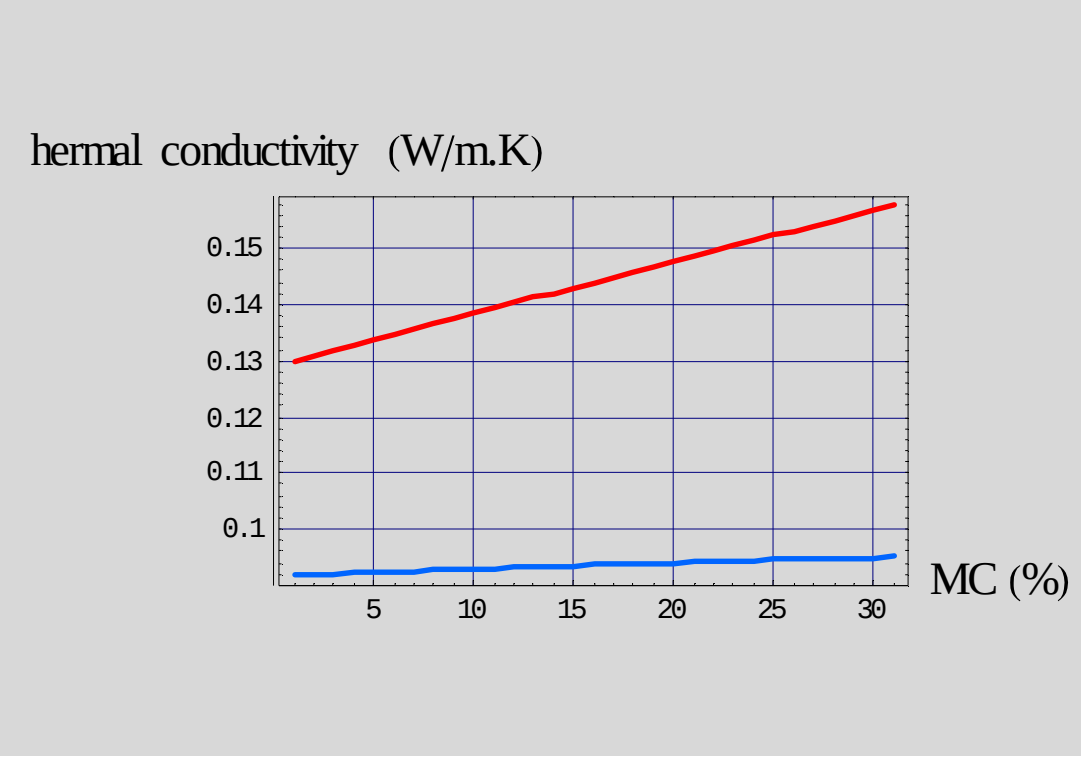

Figure 2. 36 Maple tangential (blue) and radial (red) thermal conductivity change in the range of moisture content from 0% to 30%.

From the model-predicted data and the plot, it can be found that the radial thermal conductivity of maple is significantly greater than the tangential thermal conductivity in the MC range of 0%-30%, and the radial thermal conductivity is changing faster with moisture content than the tangential thermal conductivity. Both values have a linear relationship with moisture content in the range examined. The linear relationship resulted from the relation between the cell wall substance thermal conductivity value and the MC. The ratio of radial over tangential is around 1.5 with an increase when moisture content increase from 0% to 30%. The high RTC for maple is due to the significant amount of wood rays in the species structure and being included in the model.

2.4.3.4 Comparison and Conclusion

Theoretical estimation for the thermal conductivities of two softwood species are very close because they have similar anatomical structures and same models (geometric and resistance models). Hardwood species, such as maple, have different models from the softwoods due to the anatomical structure difference.

Radial thermal conductivity is greater than tangential thermal conductivity for the species based on the model output. For softwood species, radial over the tangential thermal conductivity is due to the structure arrangement. From the geometric models (Figure 2.21), it was found that there is part of cell wall substance (sidewalls of tracheids) running through the full path of the radial heat flow, while this part of the cell wall could not be found in the tangential heat flow path (Figure 2.20). Radial thermal conductivity is about 1.2 to 2.5 times tangential thermal conductivity in the moisture content ranges from 0% to 30% and LW percentage changes from 1% to 99%. For the hardwood species, a higher radial thermal conductivity than the tangential is due to the significant amount of rays in the structure. Ray orientation and its wall substance orientation are perpendicular to the longitudinal cells in hardwood species. This ray component contributed significantly to the effective radial thermal conductivity estimated by the model.

Linear relationships were found between moisture content (in the range of 0%-30%) with radial and tangential thermal conductivities for both softwood and hardwood species. The linear relationship resulted from the linear relation between the cell wall substance thermal conductivity and moisture content in wood. Radial thermal conductivity (RTC) changes more significantly and faster with moisture content than tangential thermal conductivity (TTC) due to the structure difference in the two directions.

There is also a linear relationship between the TTC of softwood species and the LW percentage in the samples. The higher the LW% is, the higher the TTC. An inverse relationship between RTC and (1-LW) percentage on softwood species was found. The increase of RTC with the increase of LW percentage is growing followed the function of:

$$RTC = f(\frac{1}{1-LW\%})$$

Equa. (2. 19)

These relationships resulted from the different arrangement for earlywood-latewood in the radial and tangential geometric models. LW percentage affect on hardwood species was not examined in this study because the one hardwood species that was examined had insignificant and uniform latewood percent.

Two-direction thermal conductivity values in the large MC range from ovendry to saturation state were estimated by the models for softwood species -- Scots pine. Above the FSP, when free water appears in the wood sample, TTC and RTC increase dramatically with moisture content changes. No significant difference was found between TTC and RTC. The geometric difference in the two directions has little affect on the resulted thermal conductivities when free water takes part of the cell lumen.

All these conclusions were based on the theoretical model estimations. Although the geometric models and thermal resistance models were set up based on the wood anatomical structure and numerous microscopic measurements consisting of the major thermal conductivity influenced structures -- cell wall percent and latewood percent, the theoretical models are always idealized by certain assumptions. For example, in the microscopic scale, radial and tangential direction can be perfectly defined as shown in the images (Figures 2.11 to 2.18), but in the macro-scope scale of wood samples in the real world, such perfect directions can never be found. So the theoretical model outputs have to be compared with experimental results to evaluate the capability of model predictions. Validation tests for thermal conductivity measurement were preformed on the three species modeled in this study and described in the following section.